Supplementary Material

Retrospective evaluation of school-related measures on pre-vaccination transmission dynamics of SARS-CoV-2

Benedetta Canfora[1], *Rey Audie Escosio*[1,2], *Christiaan H. van Dorp*, *Otilia Boldea*, *Marc Bonten*, *Ana Nunes*, *Ganna Rozhnova*[3]

Contents

[1]These authors contributed equally and share first authorship.
[2]Corresponding author: rsescosio@alunos.fc.ul.pt
[3]Corresponding author: g.rozhnova@umcutrecht.nl.

Supplementary Section 1 Model equations and parameters

The deterministic model used in this work, and visualized in Figure 1, was formulated as a system of ordinary differential equations in Equation (1).

$$
\begin{aligned}
\frac{\mathrm{d}S_k(t)}{\mathrm{d}t} &= -\lambda_k S_k(t), \\
\frac{\mathrm{d}E_k(t)}{\mathrm{d}t} &= \lambda_k S_k(t) - \alpha E_k(t), \\
\frac{\mathrm{d}I_k(t)}{\mathrm{d}t} &= \alpha E_k(t) - (\gamma + \nu_k) I_k(t), \\
\frac{\mathrm{d}R_k(t)}{\mathrm{d}t} &= \gamma I_k(t), \\
\frac{\mathrm{d}H_k(t)}{\mathrm{d}t} &= \nu_k I_k(t),
\end{aligned}
\tag{1}
$$

We consider ten age groups denoted by k, $k = 1, \ldots, 10$. For each k, S_k represents the susceptible population, E_k represents the exposed population, I_k represents the infectious population, R_k represents the recovered population, H_k represents the hospitalized population, and N_k represents the total population i.e., $N_k = S_k(t) + E_k(t) + I_k(t) + H_k(t) + R_k(t)$. In the transmission terms of the equations, we define an age-specific force of infection λ_k equal to $\epsilon \beta_k \sum_{l=1}^{n} c_{kl}(t) \frac{I_l(t)}{N_l}$.

Supplementary Table 1. Summary of model assumptions and their justifications. This table provides an overview of the key assumptions made in the transmission model and counterfactual scenarios, along with how each was justified.

#	Assumption	Location in main text	Justification
Structural model			
1	No demographic dynamics or immunity waning	Transmission model	Analysis timeframe < 1 year; waning immunity and demographic turnover are negligible over this horizon
2	Hospitalized individuals are non-infectious	Transmission model	Small fraction at 1st wave peak (28 May 2020): hospitalized cases represented only 1% of total infections [5120 (4845–5390) vs. 358493 (273805–435534)]; strict infection control is enforced post-diagnosis
3	No explicit intra-hospital dynamics or deaths	Transmission model	Model fitted to hospitalization incidence only; nosocomial transmission is implicitly captured, as all compartments include individuals hospitalized for non-COVID conditions
4	No spatial stratification	Transmission model	Hospitalization and seroprevalence data are only available at national level
5	Alpha variant not modeled	Transmission model	First confirmed Alpha variant case in Portugal was on 21 December 2020, only 27 days before the end of the study period (15 January 2021)
Contact patterns			
6	First-lockdown contact matrix inferred from Dutch data	Data	Comparable non-pharmaceutical interventions were implemented in both countries during the first lockdown; follows Viana et al. [1]; model validity is supported by successful fitting of hospitalization and seroprevalence (Supplementary Figures 10, 11, and 12)
7	Individual measures (masks, distancing) not modeled explicitly	Transmission model	Aggregate effects captured of individual protective measures are absorbed into the estimated mitigation factor $\zeta = 0.75(0.63 - 0.87)$ and regime-specific behavioral parameters u_j (Supplementary Table 2)
8	Post-lockdown contacts modeled as linear combination of pre-pandemic and lockdown contacts	Time-varying contact patterns	Due to lack of proper data; follows Viana et al. [1]; model validity is supported by successful fitting of hospitalization and seroprevalence (Supplementary Figures 10, 11, and 12)
Data and fitting			
9	Chosen priors for transition dates between regimes	Pandemic timeline	Estimated posteriors align well within the measures implemented (Supplementary Section 2) besides Relax 2 but posteriors captured the start of uptick of cases (Figure 2); discussed extensively in Supplementary Section 6
10	Chosen log-normal priors for relative susceptibilities of 0-20 and 20-60 age groups	Parameter estimation	Following [2] with 0.23 and 0.64, respectively; weakly informative prior due to scale parameter; posteriors obtained aligns with [3]
11	Seroconversion date fixed at 28 May 2020	Parameter estimation	Sensitivity analyses for 21 Jun and 31 Jul 2020 show similar results (Supplementary Section 15, and Tables 10 and 11); conclusions qualitatively unchanged

Supplementary Table 1. (continued) Summary of model assumptions and their justifications. This table provides an overview of the key assumptions made in the transmission model and counterfactual scenarios, along with how each was justified.

#	Assumption	Location in main text	Justification
Counterfactual scenarios			
12	Non-school contacts held fixed at baseline in counterfactual scenarios	Counterfactual scenarios vs baseline	Acknowledged as a limitation in the Discussion and Supplementary Section 5; independent contributions of individual non-school measures cannot be disentangled given this modeling choice
13	Pre-pandemic contacts decompose as school + non-school	Time-varying contact patterns	Based on Mistry et al. [4] setting-specific contact matrices that provided school and overall matrices for Portugal
14	u_j applies uniformly to school and non-school contacts	Time-varying contact patterns	Alternative formulation of school contact reduction ($\zeta_s = 0.18(0.16 - 0.20)$) explored in Scenario 2.2 (Supplementary Section 17) resulting in higher hospitalizations but similar peak date (Supplementary Table 11), yet core conclusion that school closures alone cannot prevent the autumn wave is unchanged
15	Main Scenario 1 fully closes schools	Counterfactual scenarios vs baseline	Partial school mitigation levels (ξ) tested in Figure 4 and Supplementary Section 14; at $\xi \leq 0.5$, $\mathcal{R}(t)$ remains at or below 1 on 1 April 2020 and cumulative hospitalizations approach baseline; conclusions robust across all tested mitigation levels
16	Main Scenario 2 fully opens schools	Counterfactual scenarios vs baseline	Partial school mitigation levels (ξ) tested in Figure 4 and Supplementary Section 14; autumn hospitalization wave persists across all levels, as $\mathcal{R}(t)$ well above 1 at the onset of the counterfactual period; full closure reduces total cumulative hospitalizations; alternative contact formulation explored in Scenario 2.2 (Supplementary Section 17); conclusions unchanged
17	Winter school holidays have negligible impact	Time-varying contact patterns	Explicitly tested in Scenario 2.1 (Supplementary Section 17; Table 11); core conclusion that school closures alone cannot prevent the autumn wave is unchanged
18	Non-school relaxation withheld during Scenario 1	Time-varying contact patterns	Explored as pessimistic alternative to Scenario 1 in Scenario 1.1 (Supplementary Section 16; Table 10); first wave substantially exceeds observed levels in both cases
19	School opening extended through Relax 1	Time-varying contact patterns	Explored in Scenario 1.2, extending the counterfactual school opening through Relax 1 until 10 June 2020 (Supplementary Section 16; Table 10); conclusion that open schools during the first lockdown would have caused a substantially larger hospitalization wave is reinforced

Supplementary Table 2. Summary of the model parameters. This table provides an overview of all model parameters as defined in various sections of the Methods.

Description (unit)	Notation[a,b]	Median (95% CrI)	Reference
Age-independent parameters			
Probability of transmission per contact	ϵ	0.053 (0.044, 0.064)	Estimated
Initial number of infected individuals[c]	$\theta \sum_k N_k$	1,258 (819, 1,900)	Estimated
Over-dispersion parameter for the NegBinom distribution for hospitalizations	ϕ	55.64 (40.22, 80.66)	Estimated
Mitigation factor on transmission per contact after the first lockdown	ζ	0.75 (0.63, 0.87)	Estimated
Latent period (days)	$1/\alpha$	2.9 (2.2, 3.8)	Estimated
Infectious period (days)	$1/\gamma$	3.6 (3.0, 4.4)	Estimated
Age-specific parameters			
Hospitalization rates in age group k (1/day)	ν_k	$\nu_1 = 0.12\ (0.07, 0.23)$, $\nu_2 = 0.10\ (0.06, 0.21)$ $\nu_3 = 0.17\ (0.10, 0.30)$, $\nu_4 = 0.30\ (0.21, 0.43)$ $\nu_5 = 0.40\ (0.29, 0.58)$, $\nu_6 = 0.54\ (0.39, 0.79)$ $\nu_7 = 1.01\ (0.72, 1.45)$, $\nu_8 = 2.13\ (1.50, 3.03)$ $\nu_9 = 4.62\ (3.26, 6.71)$, $\nu_{10} = 14.24\ (9.91, 21.23)$	Estimated
Susceptibility of age group k relative to age group 60+, $\beta_8 = \beta_9 = \beta_{10} \equiv 1$	β_k	$\beta_1 = \beta_2 = \beta_3 = 0.48\ (0.31, 0.68)$ $\beta_4 = \beta_5 = \beta_6 = \beta_7 = 0.97\ (0.88, 0.99)$	Estimated
Population size of age group k	N_k	$N_1 = 4.3 \times 10^5$, $N_2 = 4.6 \times 10^5$ $N_3 = 1.1 \times 10^6$, $N_4 = 1.1 \times 10^6$ $N_5 = 1.3 \times 10^6$, $N_6 = 1.6 \times 10^6$ $N_7 = 1.5 \times 10^6$, $N_8 = 1.3 \times 10^6$ $N_9 = 9.7 \times 10^5$, $N_{10} = 6.7 \times 10^5$	[5]
Parameters relating to contact patterns			
Contact rate for an individual in age group k with all individuals in age group l (1/day)			
Baseline	$c_{kl}(t)$	Equation (2) and (4)	Estimated
Scenario 1	$c_{kl}(t)$	Equation (5)	Assumed
Scenario 2	$c_{kl}(t)$	Equation (5)	Assumed
Total prepandemic	b_{kl}	Fig. 2	[4]
School-based prepandemic	s_{kl}	Fig. 2	[4]
First lockdown (1/day)	a_{kl}	Fig. 2	Calibrated; [6]
Mid-point time of transition to regime j (days)	t_j[c]	$t_0 = 28\ (27, 29)$, $t_1 = 63\ (61, 66)$ $t_2 = 179\ (177, 182)$, $t_3 = 261\ (258, 264)$ $t_4 = 297\ (294, 300)$	Estimated
Speed of transition to regime j (1/day)	K_j	$K_0 = 0.9\ (0.4, 3.3)$, $K_1 = 1.3\ (0.4, 4.6)$ $K_2 = 1\ (0.3, 3.8)$, $K_3 = 0.6\ (0.3, 3.3)$ $K_4 = 0.9\ (0.3, 3.9)$	Estimated
Proportion of time an individual behaves as before the pandemic in regime $(j+1)$	u_{j+1}	$u_1 = 0.21\ (0.18, 0.24)$, $u_2 = 0.41\ (0.37, 0.46)$ $u_3 = 0.23\ (0.19, 0.28)$, $u_4 = 0.47\ (0.39, 0.55)$	Estimated
Logistic functions for transitions between regimes j	$f_j(t)$	$1/\left[1 + e^{-K_j(t-t_j)}\right]$	Estimated

Notes:
[a] Indices k and l denote age groups, where $k, l = 1, \ldots, 10$ and $n = 10$ represents the total number of age groups. These indices correspond to the following age groups: $[0, 5)$, $[5, 10)$, $[10, 20)$, $[20, 30)$, $[30, 40)$, $[40, 50)$, $[50, 60)$, $[60, 70)$, $[70, 80)$, and 80+ years.
[b] The index j denotes regimes j, $j = 0, 1, 2, 3, 4$, as defined in the section on contact rates.
[c] Time $t = 0$ corresponds to 26 February 2020.

Supplementary Section 2 Measures introduced in Portugal

Supplementary Table 3. Timeline of interventions and notable events in Portugal. This table provides an overview of select interventions and notable events regarding the pre-vaccination period of the pandemic in Portugal.

Code	Date	Description	Reference
0. First lockdown (LD 1)			
0.A	2 March 2020	First confirmed case	
0.B	13 March 2020	Declaration of a state of alert	[7]
0.C	16 March 2020	Implementation of a state of alert	[7]
		First confirmed disease-induced death	
0.D	18 March 2020	Declaration of the State of Emergency	[8]
0.E	22 March 2020	Implementation of the State of Emergency	[9]
0.F	2 April 2020	Extension of the State of Emergency	[10]
1. Relaxation after the first lockdown (Relax 1)			
1.A	17 April 2020	Regulation of the extension of the State of Emergency	[11]
		Recommendations to prepare for reopening higher education and scientific institutions	[12]
1.B	30 April 2020	Recommendations of a general deconfinement plan	[13]
		Declaration of transition to State of Calamity	[14]
1.C	3 May 2020	Implementation of the State of Calamity	[14]
1.D	18 May 2020	Resumption of in-person classes for some secondary grades	[15]
2. Further relaxation (Relax 2)			
2.A	14 August 2020	Extension of the situation of contingency and alert to 31 August 2020	[16]
2.B	28 August 2020	Extension of the situation of contingency and alert to 15 September 2020	[17]
2.C	2 September 2020	Start of private school reopening	[18]
2.D	11 September 2020	Declaration of the State of Contingency	[19]
2.E	14 September 2020	Start of public school reopening	[18]
2.F	15 September 2020	Implementation of the State of Contingency	[19]
3. Second lockdown (LD 2)			
3.A	14 October 2020	Declaration and immediate implementation of State of Calamity	[20]
3.B	2 November 2020	Extension of State of Calamity	[21]
3.C	6 November 2020	Declaration of State of Emergency	[21]
3.D	9 November 2020	Implementation of State of Emergency	[22]
3.E	20 November 2020	Extension of State of Emergency	[23]
3.F	24 November 2020	Implementation of extension of State of Emergency	[24]
1. Relaxation after the second lockdown (Relax 3)			
4.A	4 December 2020	Extension of State of Emergency	[25]
4.B	9 December 2020	Implementation of extension of State of Emergency	[26]
4.C	17 December 2020	Extension of State of Emergency	[27]
4.D	21 December 2020	First confirmed case of Alpha variant	
4.E	24 December 2020	Implementation of extension of State of Emergency	[28]
4.F	27 December 2020	Start of vaccination programs	
4.G	6 January 2021	Extension of State of Emergency	[29]
4.H	8 January 2021	Implementation of extension of State of Emergency	[30]
4.I	13 January 2021	Extension of State of Emergency	[31]
4.J	15 January 2021	Implementation of extension of State of Emergency	[32]

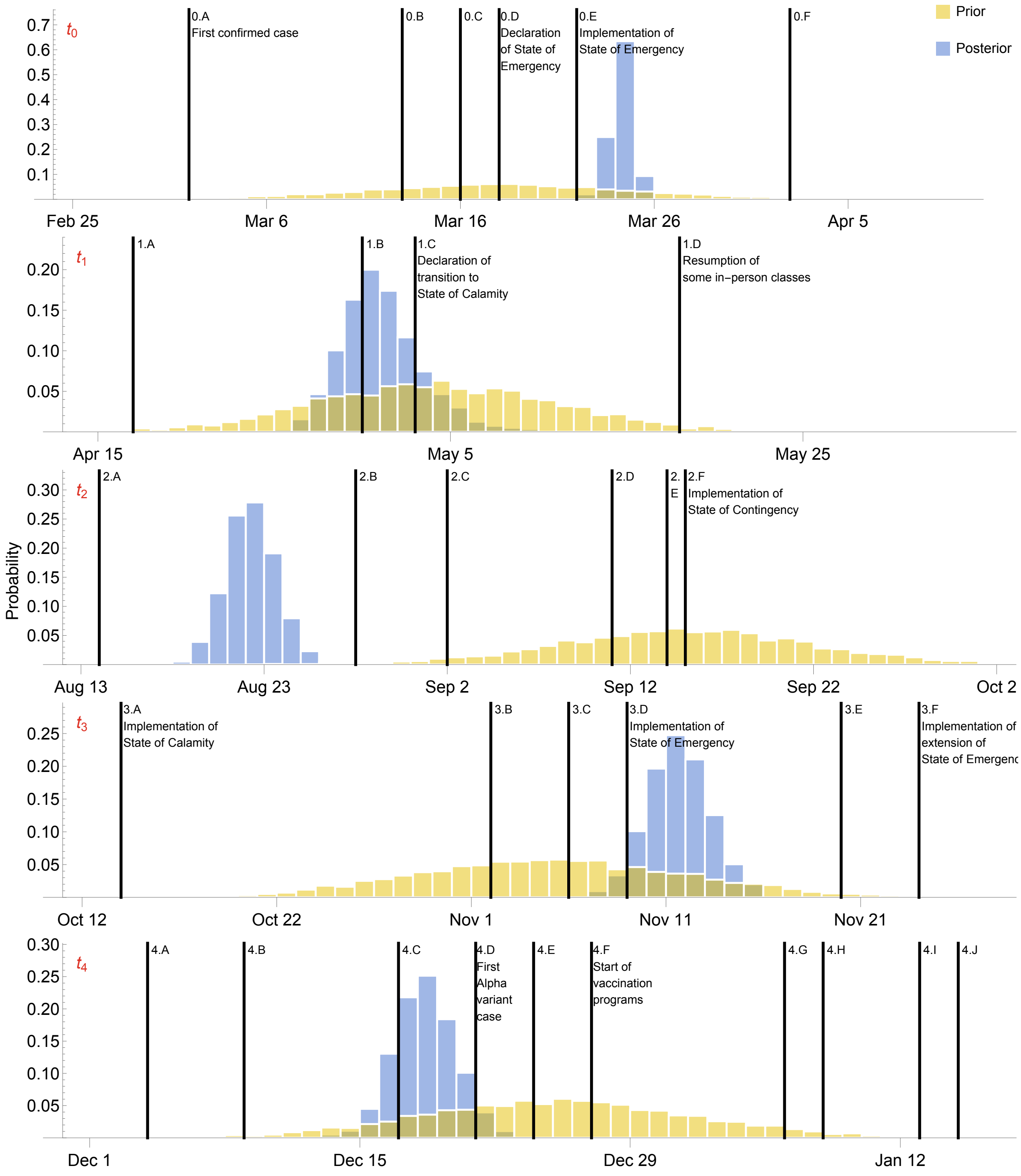

Supplementary Figure 1. Interventions and notable events in Portugal alongside estimated regime-specific times of transition, t_j. The (yellow) priors and (blue) posteriors for the regime-specific mid-point time of transition between regimes, t_j, where $j = 0, \ldots, 4$. Annotated in codes from Table 3 and black lines are interventions and notable times during the pre-vaccination period in Portugal.

Supplementary Section 3 Summary of some relevant literature on school closures

Supplementary Table 4. Summary of selected studies on school closures and reopenings. This table provides an overview of the literature used for our review, including study designs, settings, and main focus. The first column indicate the number of the reference in the main text.

#	Authors	Title	Journal, Year, Country	About
7	Ken Rice et al. [33]	Effect of school closures on mortality from coronavirus disease 2019: old and new predictions	The BMJ, 2020, UK	The study focuses on the United Kingdom (∼70 million population), using data available as of March 2020, with simulations spanning 800 days from January 1, 2020, and intervention periods of approximately 3 months (91 days). Independent replication and validation of the Imperial College London individual-based model (IBMIC) using CovidSim to simulate virus spread and assess the impact of non-pharmaceutical interventions on mortality.
8	Ganna Rozhnova et al. [34]	Model-based evaluation of school- and non-school-related measures to control the COVID-19 pandemic	Nature Communications, 2021, The Netherlands	Mathematical modeling study using an age-structured deterministic SEIR model, fitted in a Bayesian framework to hospitalization and seroprevalence data from the first wave (Feb–Apr 2020), with scenarios for August and November 2020. The analysis focuses on contact patterns, distinguishing between school settings (primary and secondary schools) and non-school settings (households and community contacts).
9	Sebastian Walsh et al. [35]	Do school closures and school reopenings affect community transmission of COVID-19? A systematic review of observational studies	BMJ, 2021, multiple countries	Systematic review of observational (mainly ecological) studies assessing the impact of school closures and reopenings on SARS-CoV-2 transmission, including studies published in 2020–2021 with data up to January 2021. The analysis focuses on school settings (nurseries, primary and secondary schools) and their effects on community transmission outcomes (infection rates, hospitalizations, and mortality).
10	Hannah Littlecott et al. [36]	Measures implemented in the school setting to contain the COVID-19 pandemic	National Library of Medicine, 2024, multiple countries	Cochrane systematic review (update of a rapid review) including only real-world empirical studies, explicitly excluding modeling studies, with evidence up to February 2022. The analysis focuses on school settings (K–12) and their impact on students, staff, households, and the broader community.
11	Jasmina Panovska-Griffiths et al. [37]	Determining the optimal strategy for reopening schools, the impact of test and trace interventions, and the risk of occurrence of a second COVID-19 epidemic wave in the UK: a modelling study	The Lancet, 2020, UK	Stochastic agent-based modeling study (using Covasim) to assess the effectiveness of testing, tracing, and isolation strategies in the context of school reopening, calibrated on UK data from January–June 2020 with projections through December 2021. The analysis is set in the United Kingdom and incorporates contact structures across households, schools, workplaces, and community settings.

Supplementary Table 4. (continued) Summary of selected studies on school closures and reopenings. This table provides an overview of the literature used for our review, including study designs, settings, and main focus. The first column indicate the number of the reference in the main text.

#	Authors	Title	Journal, Year, Country	About
12	Arden Baxter et al. [38]	Evaluating scenarios for school reopening under COVID19	BMC Public Health, 2022, USA (Georgia)	Agent-based simulation study projecting the impact of different school reopening strategies, covering the period from February 18 to November 24, 2020. Conducted in Georgia (USA), the analysis models interactions across households, K–12 schools, workplaces, and community settings.
13	Romain Ragonnet et al. [39]	Estimating the impact of school closures on the COVID-19 dynamics in 74 countries: A modelling analysis	PLoS Medicine, 2025, 74 countries	Semi-mechanistic mathematical modeling study using simulations to compare observed scenarios with counterfactual "schools open" scenarios over 2020–2022. Conducted across 74 countries, modeling contact structures in households, schools, workplaces, and community settings.
14	Benjamin Lee et al. [40]	Modeling the impact of school reopening on sars-cov-2 transmission using contact structure data from Shanghai.	BMC Public Health, 2020, China (Shanghai)	Age-structured mathematical modeling study (SIR/SEIR-type) assessing the impact of school reopening on the basic reproduction number (R_0), based on contact data from Shanghai (early 2020). The analysis focuses on age-specific contact patterns across schools, households, and community/social settings.
15	Steven Abrams et al. [41]	Modelling the early phase of the Belgian COVID-19 epidemic using a stochastic compartmental model and studying its implied future trajectories	Epidemics, 2021, Belgium	Age-structured stochastic SEIR modeling study, calibrated in a Bayesian (MCMC) framework using hospitalization, mortality, and seroprevalence data from Belgium (March–May 2020), with projections through December 2020. The analysis models interactions across households, schools, workplaces, transport, and leisure/community settings.
16	Mark M Dekker et al. [42]	Reducing societal impacts of SARS-CoV-2 interventions through subnational implementation	eLife, 2023, The Netherlands	Stochastic agent-based SEIR modeling study comparing the epidemiological and social impact of national versus subnational interventions during the first COVID-19 wave in the Netherlands (Feb 27–June 1, 2020). The analysis models interactions across 380 municipalities, distinguishing contacts in home, school, work, and community/other settings.
17	Pei Yuan et al. [43]	School and community reopening during the covid-19 pandemic: a mathematical modelling study.	Royal Society Open Science, 2022, Toronto	Deterministic compartmental modeling study (S-E-A-I-R-D) structured by age, household, and context, using data from July 31 to November 23, 2020 to assess the impact of school reopening. Conducted in Toronto (Canada), the analysis models interactions across households, schools, and community settings (including in-person work and remote work).

Supplementary Table 4. (continued) Summary of selected studies on school closures and reopenings. This table provides an overview of the literature used for our review, including study designs, settings, and main focus. The first column indicate the number of the reference in the main text.

#	Authors	Title	Journal, Year, Country	About
18	Kiesha Prem et al. [44]	The effect of control strategies to reduce social mixing on outcomes of the COVID-19 epidemic in Wuhan, China: a modelling study	National Library of Medicine, 2020, China (Wuhan)	Age-structured deterministic SEIR modeling study simulating the impact of physical distancing measures on virus transmission, with projections over one year (late 2019–end of 2020). The analysis uses contact matrices across households, schools, workplaces, and community (other) settings.
19	Lasser [45]	Assessing the impact of SARS-CoV-2 prevention measures in Austrian schools using agent-based simulations and cluster tracing data.	Nature Communications, 2022, Austria	Agent-based epidemiological modeling study calibrated with real cluster-tracing data (616 clusters, weeks 36–45 of 2020) to assess the effectiveness of NPIs, with simulations adapted to the Delta variant scenario. The analysis focuses on Austrian school settings (primary, lower and upper secondary, with/without after-school care) and households, modeling contacts among students, teachers, and relatives.
20	Leng [46]	Quantifying pupil-to-pupil SARS-CoV-2 transmission and the impact of lateral flow testing in English secondary schools.	Nature Communications, 2022, England	Stochastic individual-based modeling study, Bayesian-calibrated using PCR/LFT testing data and school absence records, covering August 31, 2020 to May 23, 2021. The analysis focuses on secondary schools in England, modeling interactions among students (close contacts, year groups) and case importation from the local community.
21	Elisabetta Colosi et al. [47]	Proactive vs. reactive COVID-19 screening in schools: lessons from experimental protocols in France during the Delta and Omicron waves	medRxiv, 2025, France	Stochastic agent-based modeling study using empirical contact data to compare weekly screening versus reactive strategies during the Delta (Nov–Dec 2021) and Omicron (Jan–Feb 2022) waves. The analysis focuses on primary school settings in France (ages 6–10), modeling within-class transmission and community-introduced cases.
22	McGee [48]	Model-driven mitigation measures for reopening schools during the covid-19 pandemic.	PNAS, 2021, USA	Stochastic network-based SEIR modeling study simulating transmission dynamics and the effectiveness of mitigation measures over a 150-day school semester (parameters reflecting 2021 variants). The analysis focuses on primary and secondary schools, modeling interactions among students, teachers, and staff within classes, social groups, and households.
23	Lessler [49]	Household covid-19 risk and in-person schooling	Science, 2021, USA	Statistical analysis of a large online survey (COVID-19 Symptom Survey via Facebook), using sampling weights and regression models to estimate adjusted odds ratios during Nov–Dec 2020 and Jan–Feb 2021. Conducted across the United States, the analysis focuses on households with in-person schooling (K–12) and teachers, assessing associated infection risks.

Supplementary Table 4. (continued) Summary of selected studies on school closures and reopenings. This table provides an overview of the literature used for our review, including study designs, settings, and main focus. The first column indicate the number of the reference in the main text.

#	Authors	Title	Journal, Year, Country	About
24	Heinsohn [50]	Infection and transmission risks of COVID-19 in schools and their contribution to population infections in Germany: A retrospective observational study using nationwide and regional health and education agency notification data	PLOS Medicine, 2022, Germany	Retrospective observational study combining descriptive infection risk analysis, multiple linear regression to assess control measures, and SEIRS compartmental modeling, covering March 2020 to April 2022 (wild-type to Omicron). Conducted in Germany (national and regional data), the analysis focuses on schools (students and teachers), households, and community settings.
25	Elisabetta Colosi et al. [51]	Modelling COVID-19 in school settings to evaluate prevention and control protocols	Anaesthesia Critical Care & Pain Medicine, 2022, France	Stochastic agent-based modeling study using empirical contact data to assess the impact of different control protocols over 90-day simulations under a Delta-wave scenario. The analysis focuses on a primary school setting (ages 6–11) in Lyon, France, modeling within-school contact networks and community-introduced cases.
26	Elisabetta Colosi et al. [52]	Screening and vaccination against COVID-19 to minimise school closure: a modelling study	The Lancet, 2022, France	Stochastic agent-based modeling study integrating empirical contact data with cost–benefit analysis of intervention protocols, calibrated on Alpha wave data (France, Mar–Jun 2021) and extended to Delta and Omicron scenarios. The analysis focuses on primary and secondary schools in France, modeling detailed contact networks between students and teachers and community-introduced cases.
27	Benjamin Faucher et al. [53]	Agent-based modelling of reactive vaccination of workplaces and schools against COVID-19	Nature Communications, 2022, France	Stochastic agent-based modeling study comparing reactive versus mass vaccination strategies, calibrated on Delta variant dynamics (autumn 2021) with simulations over a two-month period. The analysis is set in Metz (France), modeling interactions across schools (12+), universities, workplaces, households, transport, and community settings.
28	Laura Di Domenico et al. [54]	Modelling safe protocols for reopening schools during the COVID-19 pandemic in France	Nature Communications, 2021, France	Retrospective (ex-post) data-driven analysis calibrated on the first wave (up to April 2020), with projections covering the post-lockdown period from May 11 to August 2020. Conducted in Île-de-France (France), the analysis models contacts across households, schools (from preschool to high school), workplaces, transport, and leisure/community settings.
29	Thi Mui Pham et al. [55]	Seasonal patterns of sars-cov-2 transmission in secondary schools: a modelling study.	medRxiv, 2022, The Netherlands	Agent-based modeling study simulating Omicron transmission dynamics and evaluating the effectiveness of control interventions over a 30-month period starting January 3, 2022. The analysis focuses on secondary school settings (Netherlands), modeling interactions between students and teachers, including in-school contacts, leisure contacts, and community introductions.

Supplementary Section 4 Contact matrices

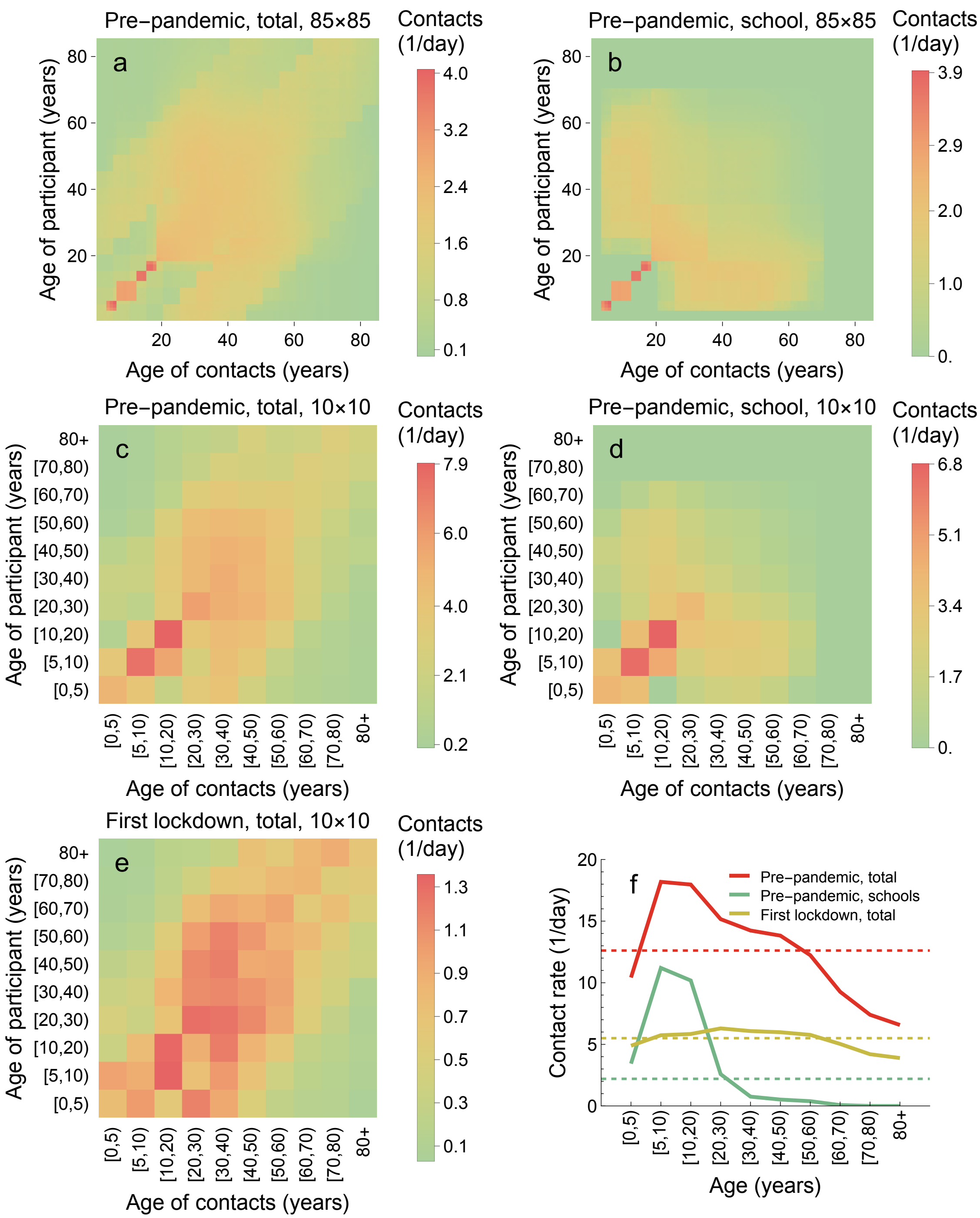

Supplementary Figure 2. Contact matrices. The 86 × 86 pre-pandemic contact matrices for (**a**) total and (**b**) school-based contacts were taken from Mistry et al [4]. Using the Portuguese demographic data, we obtained the coarse-grained 10 × 10 pre-pandemic contact matrices for (**c**) total and (**d**) school-based contacts. Due to the lack of contact data for Portugal during the first lockdown, such as that provided by Mistry et al [4] for the pre-pandemic period, we followed our previous approach [1] and inferred the Portuguese total contact matrix for this period (**e**) using data from the Netherlands [6], where a comparable set of interventions was implemented. The average number of contacts for an individual in a given age group for the three 10 × 10 contact matrices are shown in (**f**).

Supplementary Table 5. Overview of contact data considered for this study. The study period spans March 2020 to January 2021. Portugal was not included in POLYMOD (Mossong et al., 2008), the primary source of pre-pandemic empirical contact data in Europe.

Source	Country	Type	Age groups covered	Role in study
Mistry et al. [4]	Portugal (synthetic)	Pre-pandemic (pre-2020), inferred from demographic data	Fine-grained (0–80+ years)	Used: pre-pandemic baseline contact matrix for Portugal
Prem et al. [56]	Portugal (synthetic)	Pre-pandemic (pre-2020), projected	Coarse-grained (0–80+ years)	Not used: alternative pre-pandemic source; yields qualitatively similar age structure to Mistry et al. but lower resolution
Backer et al. [6]	Netherlands (empirical)	Pandemic (Mar–Jun 2020), survey-based	Coarse-grained (0–80+ years)	Used: lockdown-to-pre-pandemic contact ratio applied to the Portuguese baseline matrix, to approximate pandemic contact reductions in the absence of Portuguese-specific data
Wong et al. [57]; Verelst et al. [58]	Portugal (empirical)	Pandemic (Dec 2020 – Apr 2021), survey-based	Coarse-grained (20+ years)	Not used: overlaps with only the final weeks of the study period; does not cover individuals under 20 years, the age group central to the school closure analysis

Supplementary Section 5 Time-varying contact patterns

Scenario 1 versus baseline

For the period from 26 February to 15 July 2020, the baseline contact rate was estimated as follows

$$c_{kl}(t) = [1 - f_0(t)] \underbrace{b_{kl}}_{\substack{\text{pre-pandemic period} \\ \text{school + non-school} \\ \text{contacts}}} + f_0(t)[1 - f_1(t)] \underbrace{\zeta a_{kl}}_{\substack{\text{first lockdown} \\ \text{non-school contacts only;} \\ \text{schools closed}}} + f_1(t)[1 - f_2(t)] \underbrace{[u_1 b_{kl} + (1 - u_1)\zeta a_{kl}]}_{\substack{\text{relaxation after first lockdown} \\ \text{school + non-school contacts}}}. \tag{2}$$

Equation (2) implies that contact rates transitioned from b_{kl} before the lockdown to ζa_{kl} during the lockdown, governed by the function $f_0(t)$. For later time points, contact rates were modeled as a linear combination of b_{kl} and ζa_{kl}. Specifically, contact rates transitioned from ζa_{kl} in the lockdown to $[u_1 b_{kl} + (1 - u_1)\zeta a_{kl}]$ during the relaxation period, governed by the function $f_1(t)$. Subsequent contact modeling followed a similar approach.

In the same period, the contact rate for Scenario 1, where schools remained open instead of closing during the first lockdown, was modeled as

$$c_{kl}(t) = [1 - f_0(t)] \underbrace{b_{kl}}_{\substack{\text{pre-pandemic period} \\ \text{school + non-school} \\ \text{contacts}}} + f_0(t)[1 - f_1(t)] \underbrace{[\zeta a_{kl} + s_{kl}]}_{\substack{\text{first lockdown} \\ \text{school + non-school} \\ \text{contacts}}} + f_1(t)[1 - f_2(t)] \underbrace{[u_1 b_{kl} + (1 - u_1)\zeta a_{kl}]}_{\substack{\text{relaxation after first lockdown} \\ \text{school + non-school contacts}}}. \tag{3}$$

In Equation (3), we assumed that schools stayed open during the first lockdown with pre-pandemic levels until the first relaxation of measures. Term-by-term, Scenario 1 added pre-pandemic school contacts on top of the non-school contacts during the first lockdown.

Scenario 2 versus baseline

For the period from 15 July 2020 to 16 January 2021, the baseline contact rate was estimated as follows

$$\begin{aligned} c_{kl}(t) \quad = \quad & f_1(t)[1 - f_2(t)] \underbrace{[u_1 b_{kl} + (1 - u_1)\zeta a_{kl}]}_{\substack{\text{relaxation after first lockdown} \\ \text{school + non-school contacts}}} + f_2(t)[1 - f_3(t)] \underbrace{[u_2 b_{kl} + (1 - u_2)\zeta a_{kl}]}_{\substack{\text{further relaxation} \\ \text{school + non-school contacts} \\ \text{schools open after summer holidays}}} \\ + \quad & f_3(t)[1 - f_4(t)] \underbrace{[u_3 b_{kl} + (1 - u_3)\zeta a_{kl}]}_{\substack{\text{second lockdown} \\ \text{school + non-school contacts}}} + f_4(t) \underbrace{[u_4 b_{kl} + (1 - u_4)\zeta a_{kl}]}_{\substack{\text{relaxation after second lockdown} \\ \text{school + non-school contacts}}}. \end{aligned} \tag{4}$$

The contact rate for Scenario 2, where schools remained closed instead of reopening after the 2020 summer holidays, was modeled as

$$\begin{aligned} c_{kl}(t) \quad = \quad & f_1(t)[1 - f_2(t)] \underbrace{[u_1 b_{kl} + (1 - u_1)\zeta a_{kl}]}_{\substack{\text{relaxation after first lockdown} \\ \text{school + non-school contacts}}} + f_2(t)[1 - f_3(t)] \underbrace{[u_2 (b_{kl} - s_{kl}) + (1 - u_2)\zeta a_{kl}]}_{\substack{\text{further relaxation} \\ \text{non-school contacts only} \\ \text{schools closed after summer holidays}}} \\ + \quad & f_3(t)[1 - f_4(t)] \underbrace{[u_3 (b_{kl} - s_{kl}) + (1 - u_3)\zeta a_{kl}]}_{\substack{\text{second lockdown} \\ \text{non-school contacts}}} + f_4(t) \underbrace{[u_4 (b_{kl} - s_{kl}) + (1 - u_4)\zeta a_{kl}]}_{\substack{\text{relaxation after second lockdown} \\ \text{non-school contacts}}}. \end{aligned} \tag{5}$$

In Equation (5), we assumed that (i) the total contact rate in the pre-pandemic period, b_{kl}, was the sum of school contacts, s_{kl}, and non-school contacts, $(b_{kl} - s_{kl})$; (ii) after the 2020 summer holidays, school contacts vary regime-wise as $u_j s_{kl}$, $j = 2, 3, 4$, where u_j would also describe probability of school contacts to behave pre-pandemically; (iii) school closures can be modeled by subtracting these mitigated school contacts, $u_j s_{kl}$, thus only retaining non-school contacts from Relax 2 onwards; and (iv) the two-week school closure for winter holidays from 21 December 2020 till 3 January 2021 [18] had little impact on hospitalizations and, therefore, was not explicitly modeled. Time-varying contact patterns for the baseline versus Scenario 1 and the baseline versus Scenario 2 are shown in Supplementary Figures 3-5.

On non-school contacts

For the counterfactual scenarios, total contacts are separated into additive school and non-school components, with only school contacts varied to represent opening and closure, while non-school contacts evolve as in the baseline. This, however, assumes that non-school behavior would have been identical regardless of the school policy adopted, which may not hold in practice, as school-related measures in Portugal were consistently implemented alongside broader non-school interventions (Supplementary Section 2). Our subsequent results should therefore be interpreted in light of this assumption, acknowledging that the independent contributions of individual non-school measures cannot be disentangled.

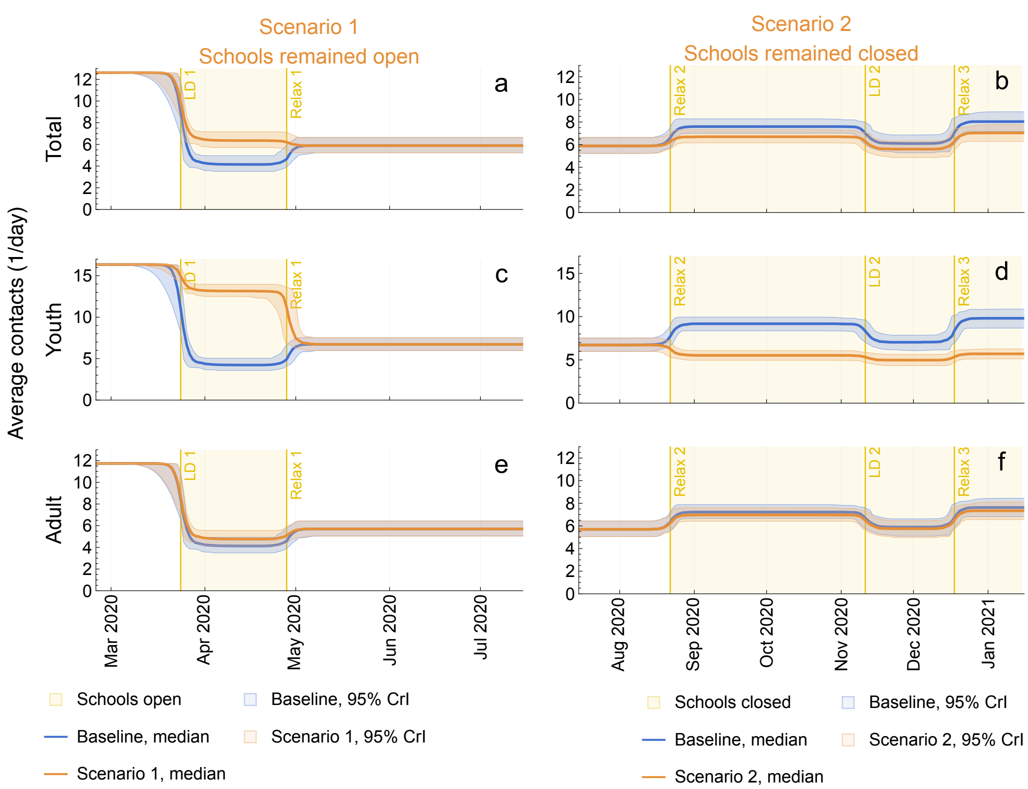

Supplementary Figure 3. Impact of scenarios on contact rates. (**a**, **b**) Total, (**c**, **d**) youth (0-20 years), and (**e**, **f**) adult (20+ years) contact rates in (**a**, **c**, **e**) Scenario 1: schools remained open instead of closing during the first lockdown in spring 2020 and (**b**, **d**, **f**) Scenario 2: schools remained closed instead of reopening after the 2020 summer holidays. The blue lines are the median trajectories estimated from the model and the blue-shaded regions correspond to the 95% CrI of the posterior predictive distribution. The orange lines and the orange-shaded regions are the respective quantities in Scenarios 1 and 2. The yellow-shaded area represents the period when schools were open (**a**, **c**, **e**) and closed (**b**, **d**, **f**) in the counterfactual scenario analyses 1 and 2, respectively. LD: lockdown. Relax: relaxation of measures.

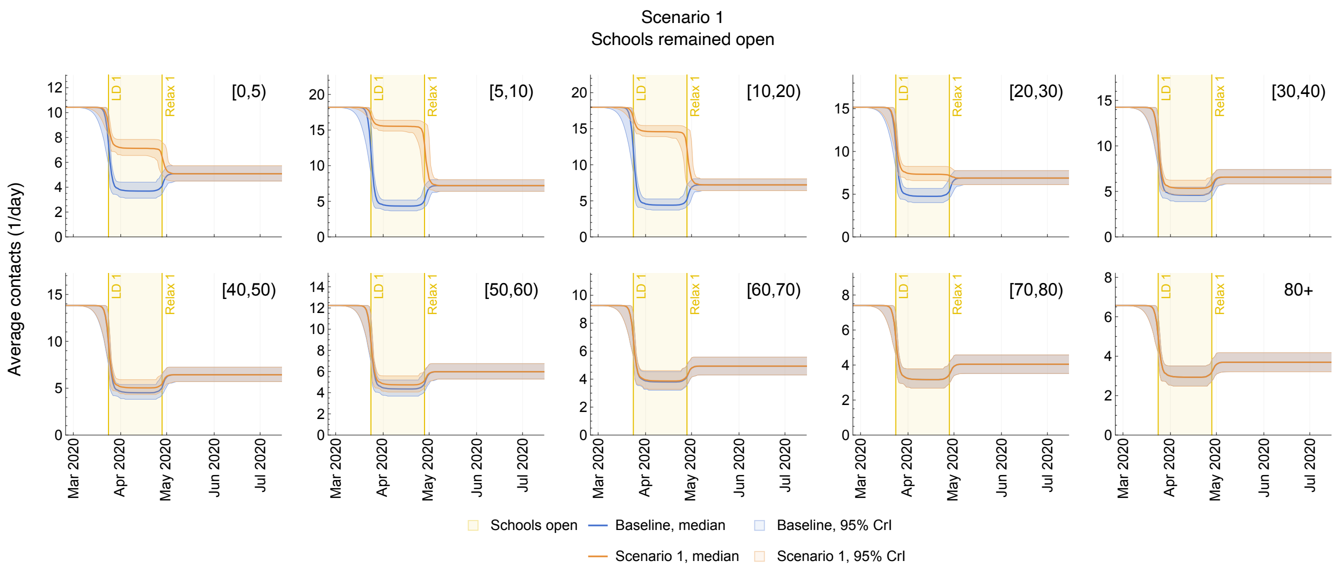

Supplementary Figure 4. Impact of Scenario 1 on contact rates in ten age groups. Contact rates in Scenario 1: schools remained open instead of closing during the first lockdown in spring 2020 for the ten age groups, as annotated. The blue lines are the median trajectories estimated from the model and the blue-shaded regions correspond to the 95% CrI of the posterior predictive distribution. The orange lines and the orange-shaded regions are the respective quantities for Scenario 1. The yellow-shaded area represents the period when schools were open in the counterfactual scenario analyses 1. LD: lockdown. Relax: relaxation of measures.

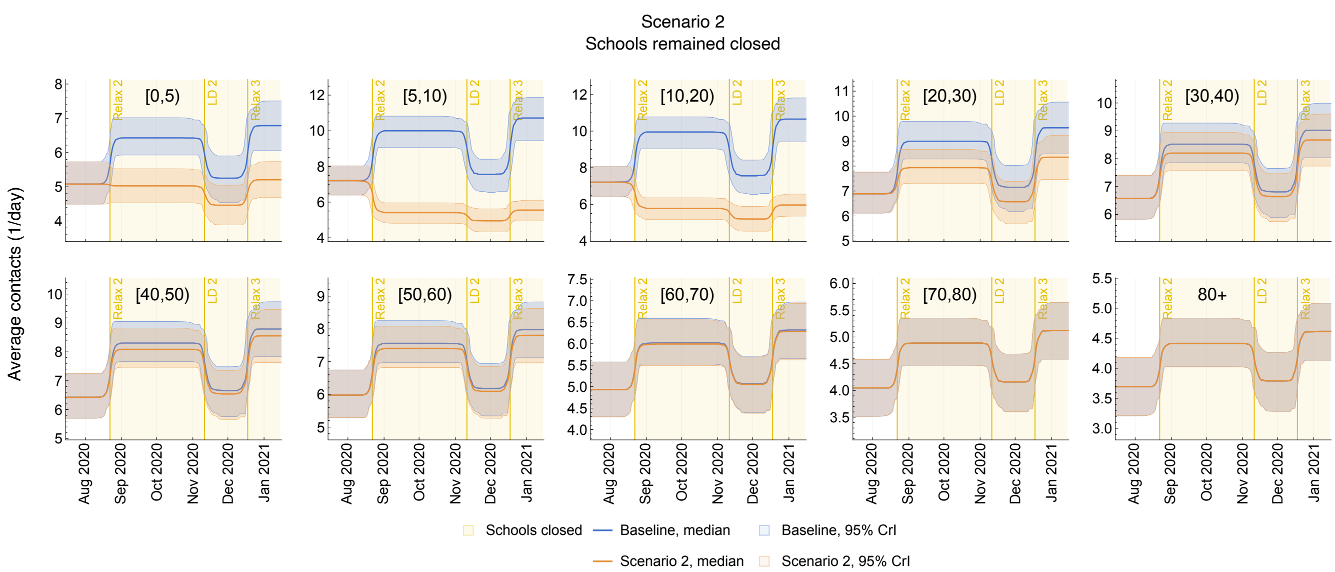

Supplementary Figure 5. Impact of Scenario 2 on contact rates in ten age groups. Contact rates in Scenario 2: schools remained closed instead of reopening after the 2020 summer holidays for the ten age groups, as annotated. The blue lines are the median trajectories estimated from the model and the blue-shaded regions correspond to the 95% CrI of the posterior predictive distribution. The orange lines and the orange-shaded regions are the respective quantities for Scenario 2. The yellow-shaded area represents the period when schools were closed in the counterfactual scenario analyses 2. LD: lockdown. Relax: relaxation of measures.

Supplementary Section 6 Parameter estimation

Prior distributions

For parameters ϵ, θ, ϕ, ν_k, and u_i we assigned vague or flat priors, meaning their posterior distributions were mostly inferred from the data. The duration of the exposed (α^{-1}) and infectious periods (γ^{-1}) had Gamma prior distributions, with 99% of the prior probability mass ranging from 2 to 5 days [59, 60] and 2.9 to 5.2 days [61], respectively. The relative susceptibilities of the 0-20 years age group, $\beta_{1,2,3}$, and of the 20-60 years age group, $\beta_{4,5,6,7}$, had log-normal prior distributions with medians 0.23 and 0.64, respectively, and a scale parameter of 0.5 [2], ensuring a weakly informative prior. The relative susceptibility of the 60+ age group was set to $\beta_{8,9,10} \equiv 1$. The transmission mitigation parameter ζ had a $\mathcal{N}(1, 0.1)$ prior reflecting the belief that reduced contacts (encoded by the contact matrix a_{kl}) were the primary determinant for the reduction in transmission during the first lockdown. The mid-point times of transition between different behavioral regimes, t_0, t_2, t_3, and t_4, were assigned normal priors with means 22, 203, 254, and 304 days post 26 February 2020, and standard deviations of 7 days, generally following the measures implemented in Portugal as shown in Table 3 and Figure 1. The time point t_1, marking the relaxation of the first lockdown, was assigned a prior distribution $\mathcal{N}(69 + 2.94/K_1, 7)$, ensuring that by 4 May 2020 the effect of the relaxation reached 5% of full uptake. Finally, the rates K_i, determining how quickly behavioral changes occurred, were given Exp(1) priors. While its mean $\mathbb{E}(K_i) = 1$ corresponds to a 6-day transition time for 5% to 95% uptake, its broad 95% credible interval of $[1.6, 176]$ days confirms it is weakly informative, thus allowing the posterior estimates to be driven by the observed data and aligning with transition ranges reported in the literature [62, 63].

Dynamical and observation model

Next, we solved the initial value problem defined by Equation (1) using the Adams-Moulton method. We recorded the state of the system at each observation time i ($i = 1, \ldots, t_{\text{data}}$), where t_{data} corresponds to the final date in the hospitalization dataset (15 January 2021). The model was fitted to hospitalization incidence data stratified by age group. Let $h_{k,i}$ denote the number of hospitalizations observed in the interval $[i-1, i)$ for age group k. The cumulative incidence of hospitalizations in this time interval was approximated as $\mu_{k,i} \equiv \nu_k I_k(i)$. We then used a negative binomial probability mass function to model the probability of the observed data, given the model prediction

$$P_{\text{hosp}}(h_{k,i} \mid \mu_{k,i}, \phi) = \binom{h_{k,i} + \phi - 1}{h_{k,i}} \left(\frac{\mu_{k,i}}{\mu_{k,i} + \phi}\right)^{h_{k,i}} \left(\frac{\phi}{\mu_{k,i} + \phi}\right)^{\phi}. \tag{6}$$

The negative binomial distribution was chosen because it allows for a larger dispersion around the mean hospitalizations compared to, for example, a Poisson distribution, allowing the model to capture large fluctuations in the hospitalization data. Relying solely on hospitalization data would have led to poor identifiability of the parameters, particularly for the hospitalization rates ν_k. Therefore, we also incorporated seroprevalence data, which was sampled around day $t_{\text{sero}} = 93$ post 26 February 2020. We neglected the waning of immunity and assumed the probability of a positive serological test for a randomly selected individual in age group k to be $p_k \equiv (1 - S_k(t_{\text{sero}})/N_k)$. The seroprevalence data was aggregated into five age groups: $[1, 10)$, $[10, 20)$, $[20, 40)$, $[40, 60)$ and 60+ years old, as available from the data [64]. To obtain the expected fraction q_k of seropositive samples in each of these age groups, we used relative population sizes. Let L_k denote the number of individuals tested in age group k and let ℓ_k represent the number of positive tests. The probability of observing ℓ_k positive tests was modeled using a binomial distribution

$$P_{\text{sero}}(\ell_k \mid L_k, q_k) = \binom{L_k}{\ell_k} q_k^{\ell_k} (1 - q_k)^{L_k - \ell_k} \,. \tag{7}$$

The total log-probability of all the hospitalization and serological data was then given by

$$\log(P_{\text{data}}) = \sum_{i=1}^{t_{\text{data}}} \sum_{k=1}^{10} \log\big(P_{\text{hosp}}(h_{k,i} \mid \mu_{k,i}, \phi)\big) + \sum_{k=1}^{5} \log\big(P_{\text{sero}}(\ell_k \mid L_k, q_k)\big) \,. \tag{8}$$

We used four parallel chains of length 1500 with a warm-up phase of length 1000, resulting in 2000 parameter samples from the posterior distribution. MCMC convergence was assessed with the $\hat{R}$ statistic (using the R `posterior` package). The value of $\hat{R}$ was below 1.01 for all parameters. For other details, see Viana et al. [1].

Estimated parameters

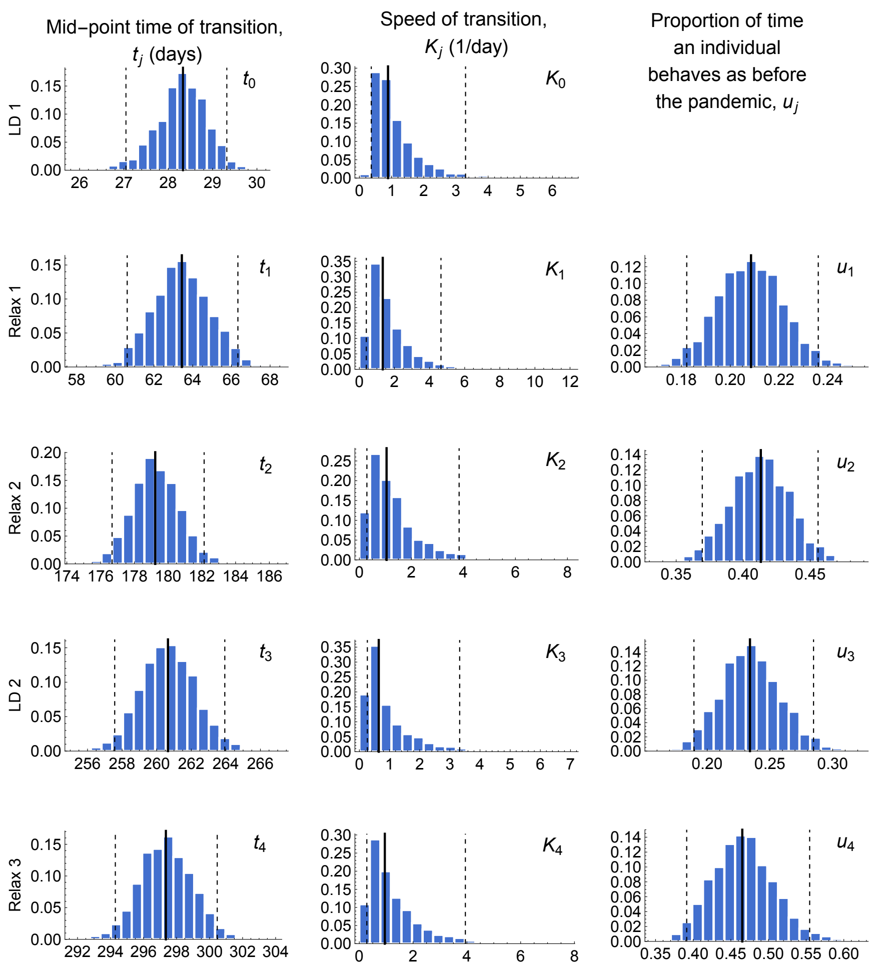

Supplementary Figure 6. Estimated parameters describing contact patterns. The histograms are based on 2000 parameter samples from the posterior distribution for the (left) mid-point time of transition to regime j, t_j, (center) speed of transition, K_j, and (right) proportion of time an individual behaves as before the pandemic in regime $(j+1)$, u_j, for each regime $j = 0, 1, 2, 3, 4$, annotated in rows. The solid and the dashed black lines correspond to the median and the 95% CrI, both of which are tabulated in Table 2. LD: lockdown. Relax: relaxation.

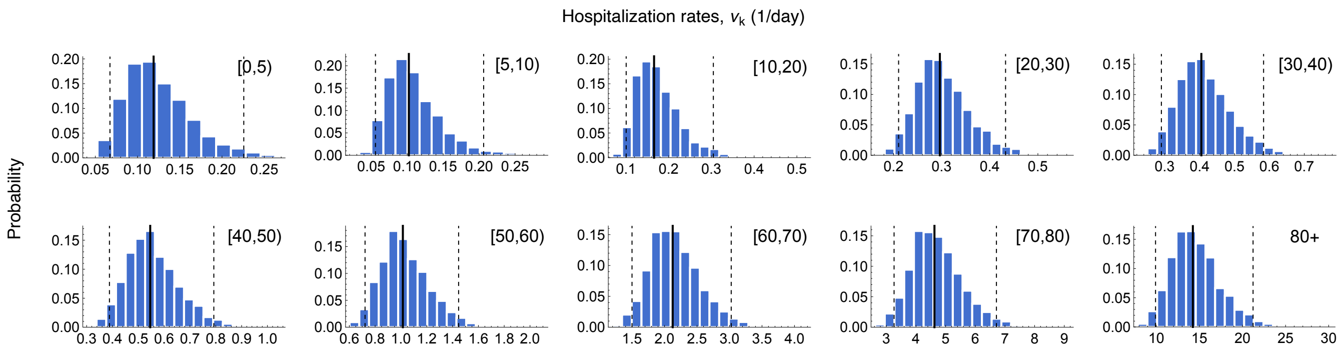

Supplementary Figure 7. Estimated hospitalization rates. The histograms are based on 2000 parameter samples from the posterior distribution for the age-specific hospitalization rate in age-group k, ν_k, where $k = 1, \ldots, 10$. The solid and the dashed black lines correspond to the median and the 95% CrI, both of which are tabulated in Table 2.

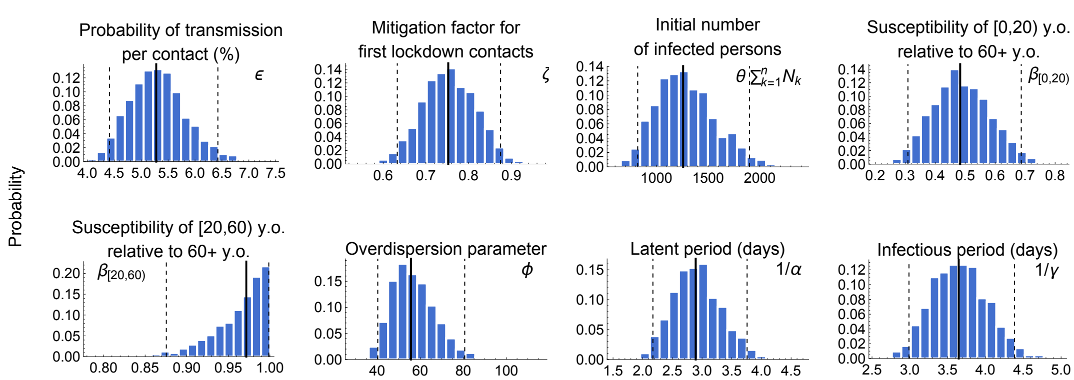

Supplementary Figure 8. Estimates of other parameters. The histograms are based on 2000 parameter samples from the posterior distribution for the estimated model parameters, each described by their respective titles. The solid and the dashed black lines correspond to the median and the 95% CrI, both of which are listed in Table 2. All parameters were estimated using a Bayesian framework, except for ζ_s, which was calibrated. For this, school contacts after the 2020 summer holidays were described by $\zeta_s s_{kl}$, where ζ_s is a mitigation factor in school transmission-relevant contacts due to the protective measures in schools and s_{kl} is pre-pandemic school contact matrix. Consequently, ζ_s was calibrated using linear programming to ensure that non-school contacts did not fall below their levels prior to the second relaxation if schools remain closed in Scenario 2.

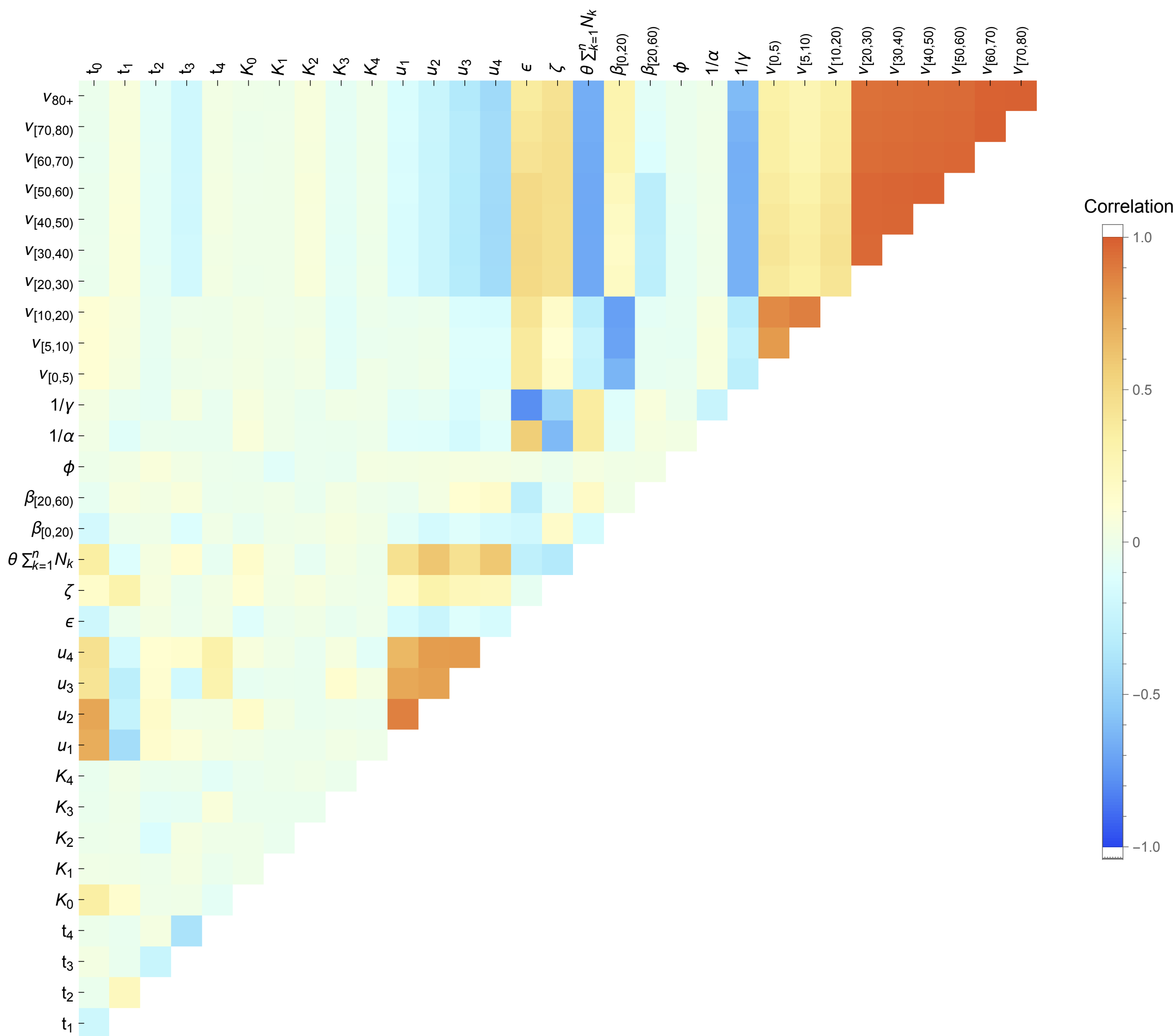

Supplementary Figure 9. Posterior correlation matrix of estimated model parameters. Each cell shows the pairwise Pearson correlation coefficient between two parameters from 2000 samples of their joint posterior distribution. Warm colors (orange–red) indicate positive correlations and cool colors (blue) indicate negative correlations with near-white cells indicate weak or negligible correlation.

Supplementary Section 7 Model fit to seroprevalence data

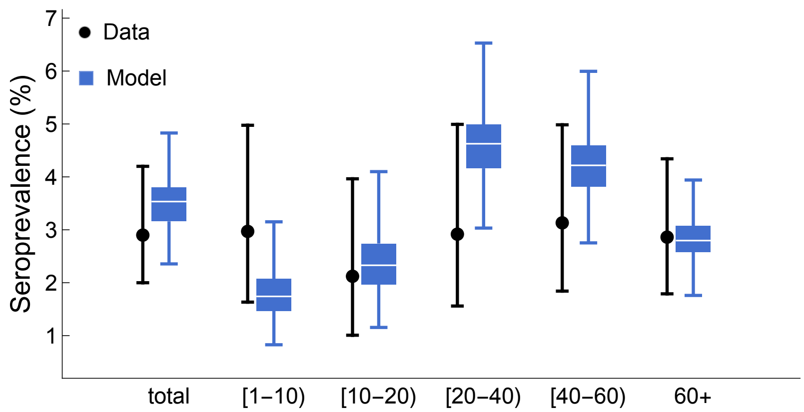

Supplementary Figure 10. Model fit to COVID-19 seroprevalence. Both total and age-specific seroprevalence are shown in the plot. The black circles with 95% confidence intervals represent the data obtained from the first serological survey (ISNCOVID-19) conducted in Portugal between 21 May 2020 and 8 July 2020 [64] used for fitting the model. The blue box plots represent the marginal posterior distribution of the seroprevalence on 28 May 2020 based on 2000 samples from the joint posterior parameter distribution.

Supplementary Section 8 Model fit to hospitalization data

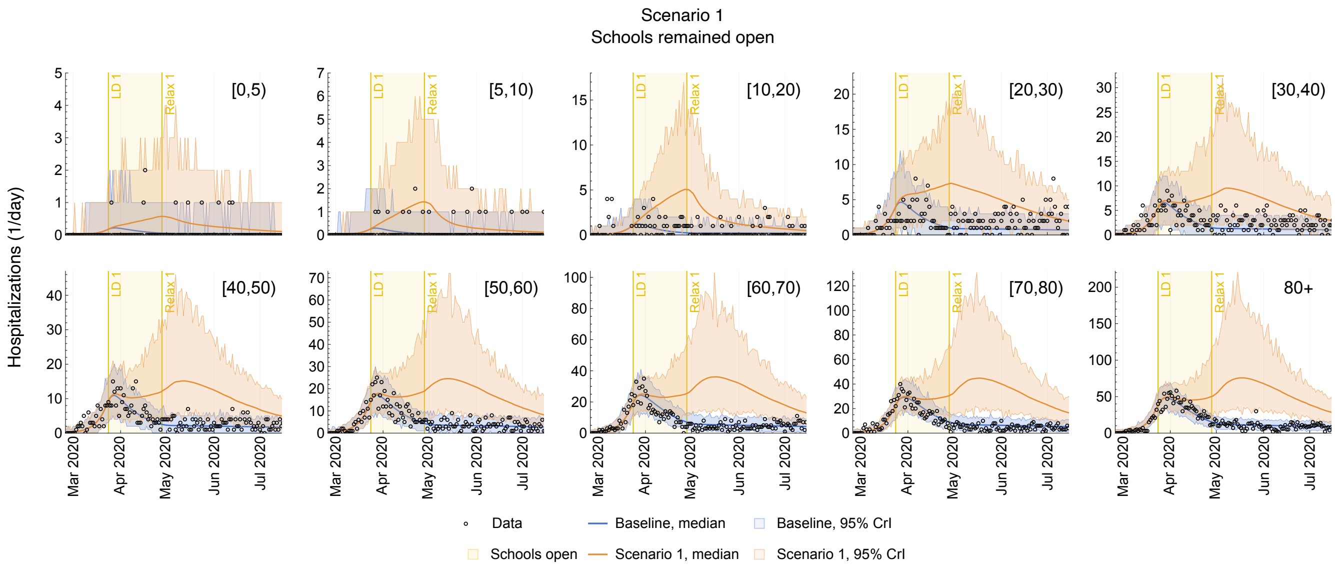

Supplementary Figure 11. Impact of Scenario 1 on age-specific hospitalizations in ten age groups. Absolut number of daily hospital admissions with COVID-19 in Scenario 1: schools remained open instead of closing during the first lockdown in spring 2020 for the ten age groups, as annotated. The circles denote daily hospital admission data. The blue lines are the median trajectories estimated from the model and the blue-shaded regions correspond to the 95% CrI of the posterior predictive distribution. The orange lines and the orange-shaded regions are the respective quantities for Scenario 1. The yellow-shaded area represents the period when schools were open in the scenario analysis. LD: lockdown. Relax: relaxation of measures.

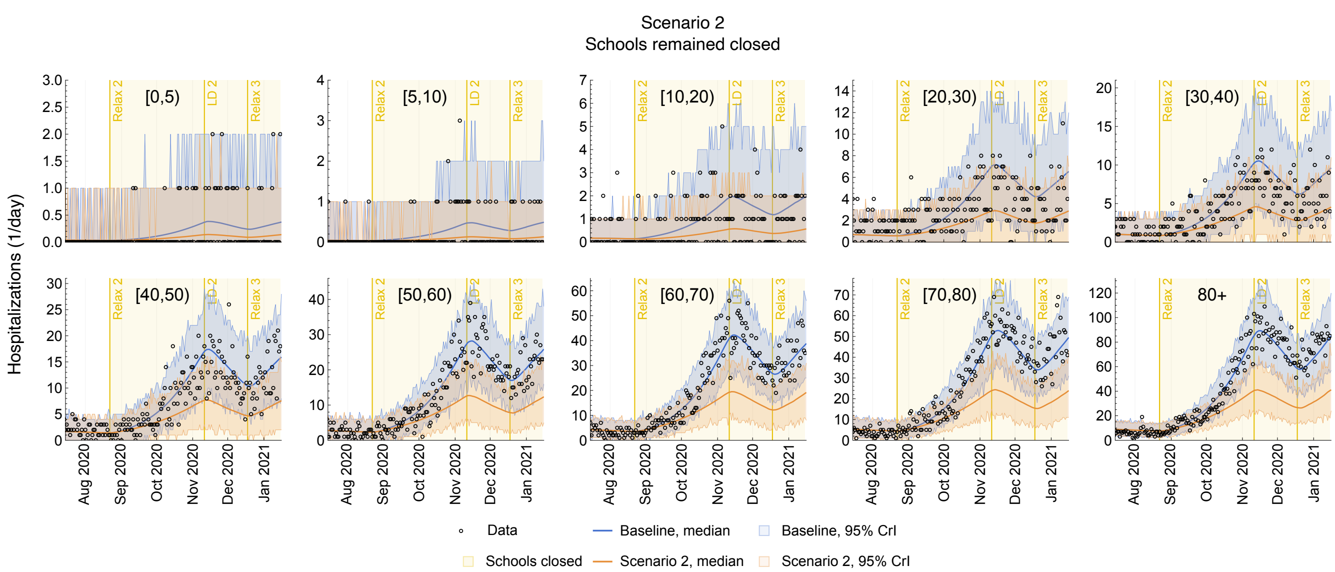

Supplementary Figure 12. Impact of Scenario 2 on age-specific hospitalizations in ten age groups. Absolute number of daily hospital admissions with COVID-19 in Scenario 2: schools remained closed instead of reopening after the 2020 summer holidays for the ten age groups, as annotated. The circles denote daily hospital admission data. The blue lines are the median trajectories estimated from the model and the blue-shaded regions correspond to the 95% CrI of the posterior predictive distribution. The orange lines and the orange-shaded regions are the respective quantities for Scenario 2. The yellow-shaded area represents the period when schools were closed in the scenario analysis. LD: lockdown. Relax: relaxation of measures.

Supplementary Section 9   Reproduction number and elasticity analysis

By following the process described in [65], we can construct the time-varying next-generation matrices [65], denoted by $K_{kl}(t)$. The elements of $K_{kl}(t)$ represent the average number of secondary infections in age group k caused by a single infectious individual in age group l at time t and is given by

$$K_{kl}(t) = \frac{\epsilon \beta_k c_{kl}(t)}{\gamma + \nu_l} \frac{S_k(t)}{N_l}\,, \tag{9}$$

where $k, l = 1, \ldots, n$ and $S_k(t)$ is given by the solution of Equation (1). The spectral radii of these $K_{kl}(t)$ comprise the time-varying effective reproduction number, $\mathcal{R}(t)$. A value of $\mathcal{R}(t) > 1$ indicates exponential growth in infections, whereas $\mathcal{R}(t) < 1$ indicates a decline.

Considering that these spectral radii have their corresponding left and right eigenvectors ($\mathbf{v}(t)$ and $\mathbf{w}(t)$ respectively), we can use elasticity analysis to obtain elasticity matrices $\mathcal{E}_{kl}(t)$. Each entry of the elasticity matrix, $\mathcal{E}_{kl}(t)$, represents the relative contribution of $K_{kl}(t)$ to $\mathcal{R}(t)$ and can be defined as follows for our model,

$$\mathcal{E}_{kl}(t) = \frac{K_{kl}(t)}{\mathcal{R}(t)} \frac{\partial \mathcal{R}(t)}{\partial K_{kl}(t)}\,. \tag{10}$$

Similar to $K_{kl}(t)$, this yields dimensions of 10×10 corresponding to each age group. With the property that $\sum_{k,l} \mathcal{E}_{kl}(t) = 1$ [66], we can construct a 2×2 elasticity matrix corresponding to adult-youth elasticities by aggregating their respective submatrices. With the property that $e_k(t) \equiv \sum_l \mathcal{E}_{kl}(t) = \sum_l \mathcal{E}_{lk}(t)$ [67], we can aggregate these values further to get age-specific cumulative elasticities,

$$e_k(t) = \sum_l \mathcal{E}_{kl}(t) = \sum_l \frac{K_{kl}(t)}{\mathcal{R}(t)} \frac{\partial \mathcal{R}(t)}{\partial K_{kl}(t)} = \sum_l \frac{K_{kl}(t)}{\mathcal{R}(t)} \frac{v_k(t) w_l(t)}{\langle \mathbf{v}(t), \mathbf{w}(t) \rangle}\,, \tag{11}$$

where $\langle \cdot, \cdot \rangle$ denotes the dot product. These $e_k(t)$ represents the relative contribution of age group k to $\mathcal{R}(t)$.

Supplementary Section 10 Age-specific contributions to $\mathcal{R}(t)$

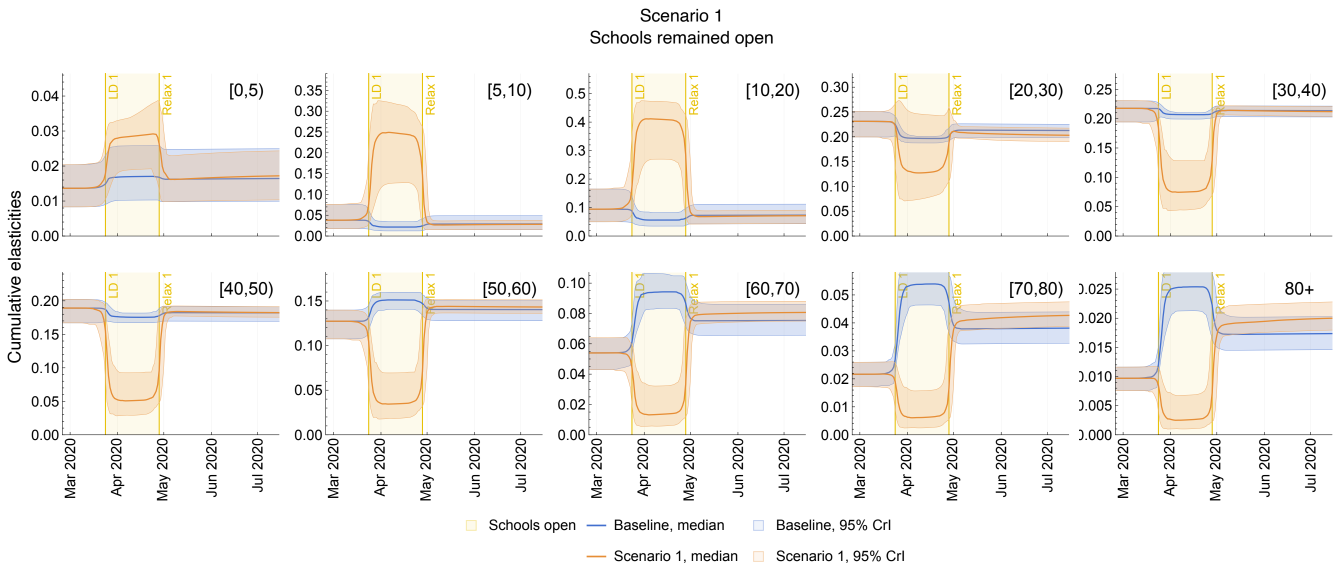

Supplementary Figure 13. Impact of Scenario 1 on the contribution of ten age groups to $\mathcal{R}(t)$. Cumulative elasticities in Scenario 1: schools remained open instead of closing during the first lockdown in spring 2020 for the ten age groups, as annotated. The blue lines are the median trajectories estimated from the model and the blue-shaded regions correspond to the 95% CrI of the posterior predictive distribution. The orange lines and the orange-shaded regions are the respective quantities for Scenario 1. The yellow-shaded area represents the period when schools were open in the scenario analysis. LD: lockdown. Relax: relaxation of measures.

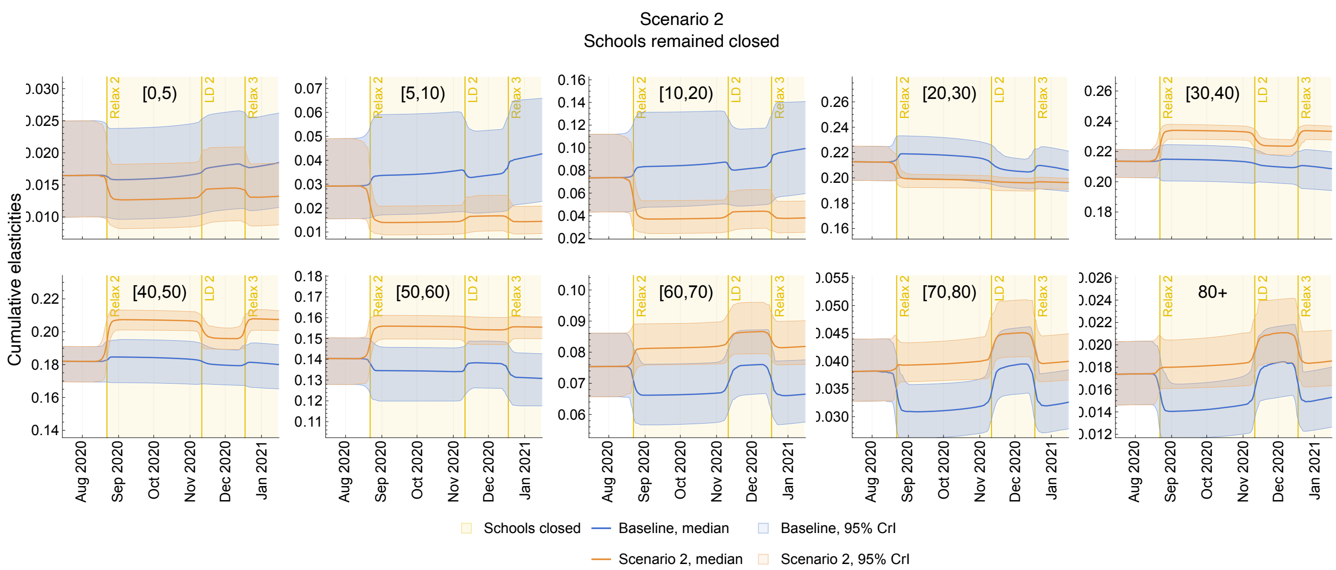

Supplementary Figure 14. Impact of Scenario 2 on the contribution of ten age groups to $\mathcal{R}(t)$. Cumulative elasticities in Scenario 2: schools remained closed instead of reopening after the 2020 summer holidays for the ten age groups, as annotated. The blue lines are the median trajectories estimated from the model and the blue-shaded regions correspond to the 95% CrI of the posterior predictive distribution. The orange lines and the orange-shaded regions are the respective quantities for Scenario 2. The yellow-shaded area represents the period when schools were closed in the scenario analysis. LD: lockdown. Relax: relaxation of measures.

Supplementary Section 11 Comparison of cumulative hospitalizations

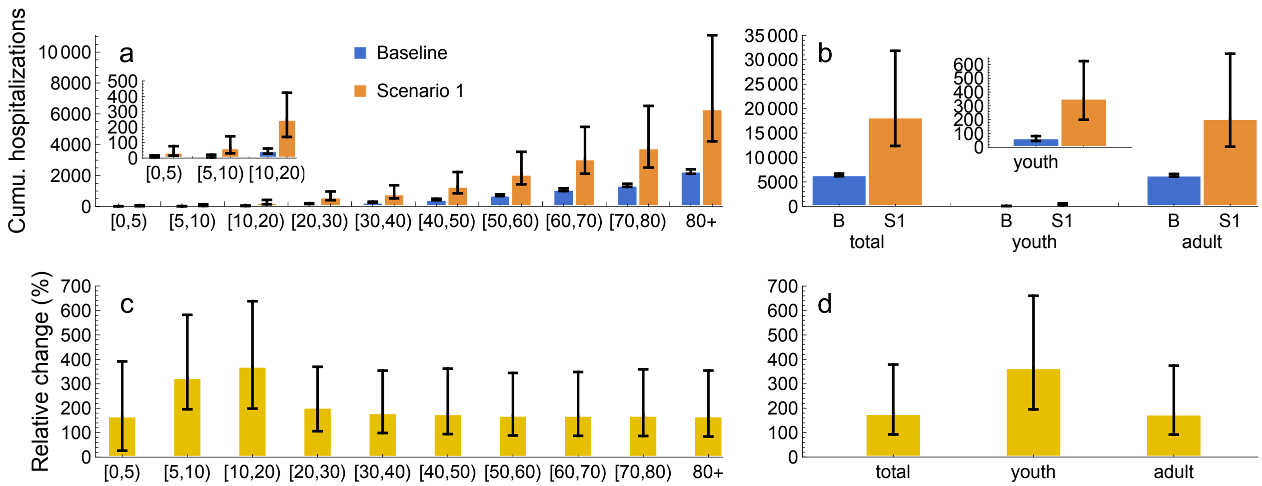

Supplementary Figure 15. Comparison of cumulative hospitalizations for Scenario 1 vs baseline. (**a**) Age-specific, (**b**) total, youth, and adult cumulative hospital admissions with COVID-19 in Scenario 1: schools remained open instead of closing during the first lockdown in spring 2020. The bar graphs are the median values obtained on 15 July 2020 and the error bars correspond to the 95% CrI of the posterior predictive distribution (based on $n = 100$ independent model runs). The insets for (**a**) and (**b**) show a close-up of the youth cumulative hospitalizations. The increase in cumulative hospitalizations for Scenario 1 relative to the baseline is shown for (**c**) age-specific, and (**d**) total, youth, and adult cumulative hospitalizations. B: baseline. S1: Scenario 1. Cumu.: cumulative.

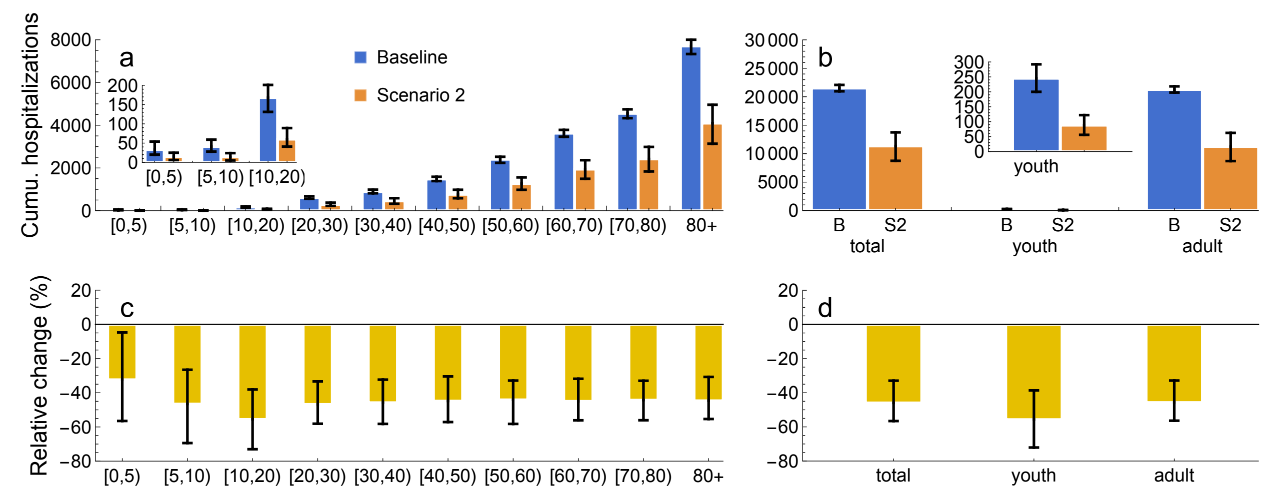

Supplementary Figure 16. Comparison of cumulative hospitalizations for Scenario 2 vs baseline. (**a**) Age-specific, (**b**) total, youth, and adult cumulative hospital admissions with COVID-19 in Scenario 2: schools remained closed instead of reopening after the 2020 summer holidays. The bar graphs are the median values obtained on 15 January 2020 and the error bars correspond to the 95% CrI of the posterior predictive distribution (based on $n = 100$ independent model runs). The insets for (**a**) and (**b**) show a close-up of the youth cumulative hospitalizations. The decrease in cumulative hospitalizations for Scenario 2 relative to the baseline is shown for (**c**) age-specific, and (**d**) total, youth, and adult cumulative hospitalizations. B: baseline. S2: Scenario 2. Cumu.: cumulative.

Supplementary Section 12 Model projections for seroprevalence

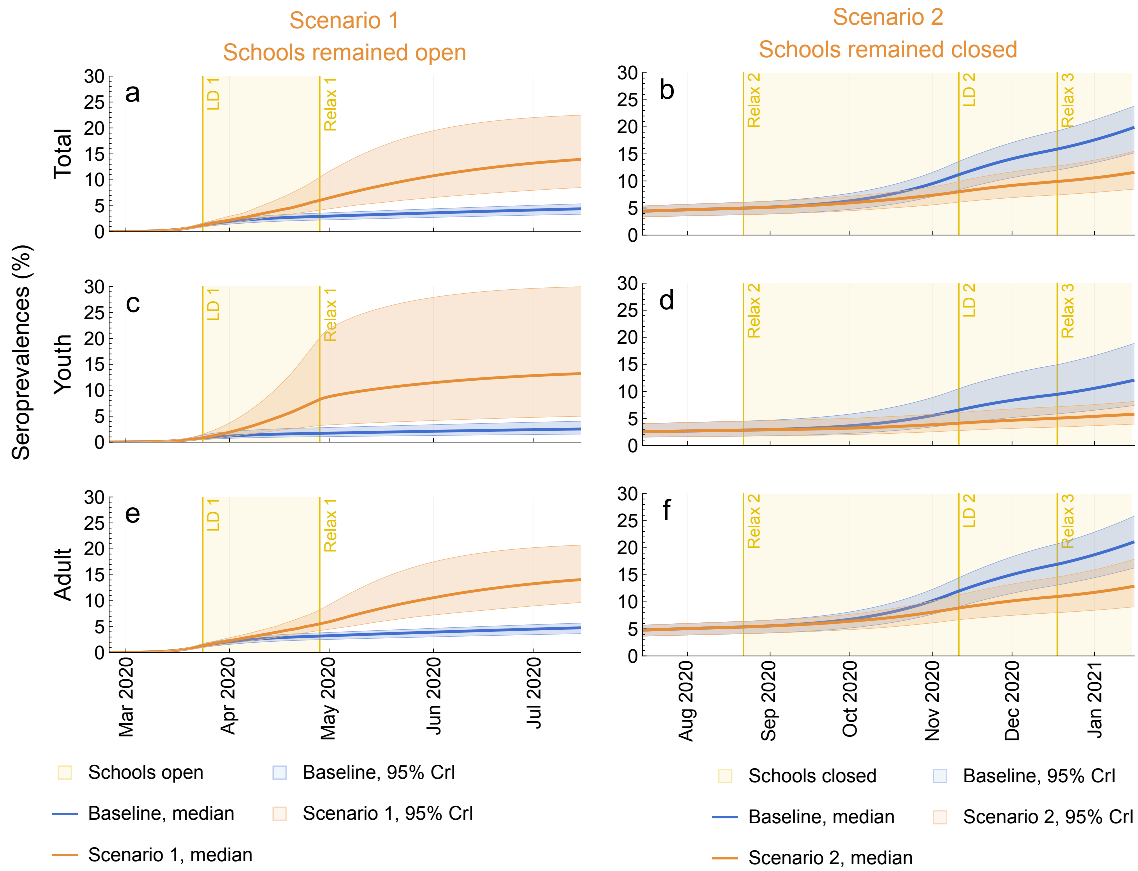

Supplementary Figure 17. Impact of scenarios on seroprevalence. (**a**, **b**) Total, (**c**, **d**) youth (0-20 years), and (**e**, **f**) adult (20+ years) seroprevalence. (**a**, **c**, **e**) Scenario 1: schools remained open instead of closing during the first lockdown in spring 2020. (**b**, **d**, **f**) Scenario 2: schools remained closed instead of reopening after the 2020 summer holidays. The blue lines are the median trajectories estimated from the model and the blue-shaded regions correspond to the 95% CrI of the posterior predictive distribution. The orange lines and the orange-shaded regions are the respective quantities for Scenarios 1 and 2. The yellow-shaded area represents the period when schools were open (**a**, **c**, **e**) and closed (**b**, **d**, **f**) in the scenario analyses 1 and 2, respectively. LD: lockdown. Relax: relaxation of measures.

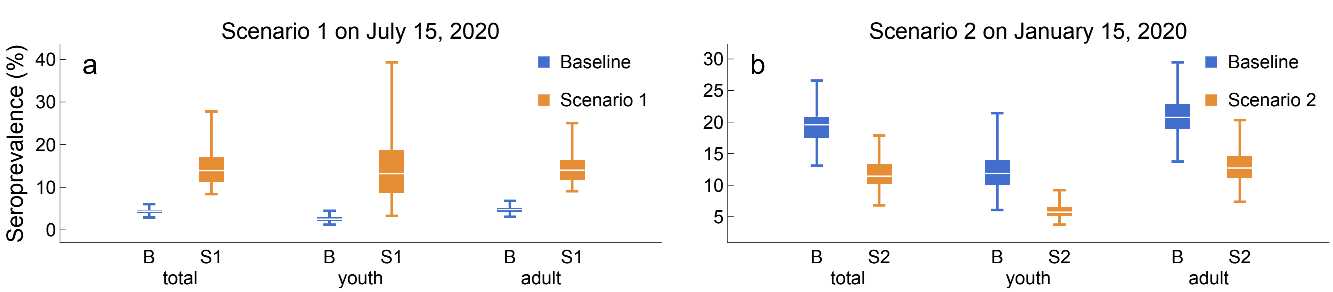

Supplementary Figure 18. Comparison of seroprevalence on scenario enddates. Total, youth (0-20 years), and adult (20+ years) seroprevalence. (**a**) Scenario 1: schools remained open instead of closing during the first lockdown in spring 2020. (**b**) Scenario 2: schools remained closed instead of reopening after the 2020 summer holidays. The box plots represent the marginal posterior distribution (based on $n = 100$ independent model runs) of the seroprevalence on (**a**) 15 July 2020 and (**b**) 15 January 2020. B: baseline. S1: Scenario 1. S2: Scenario 2.

Supplementary Section 13 Uncertainty in the model projections

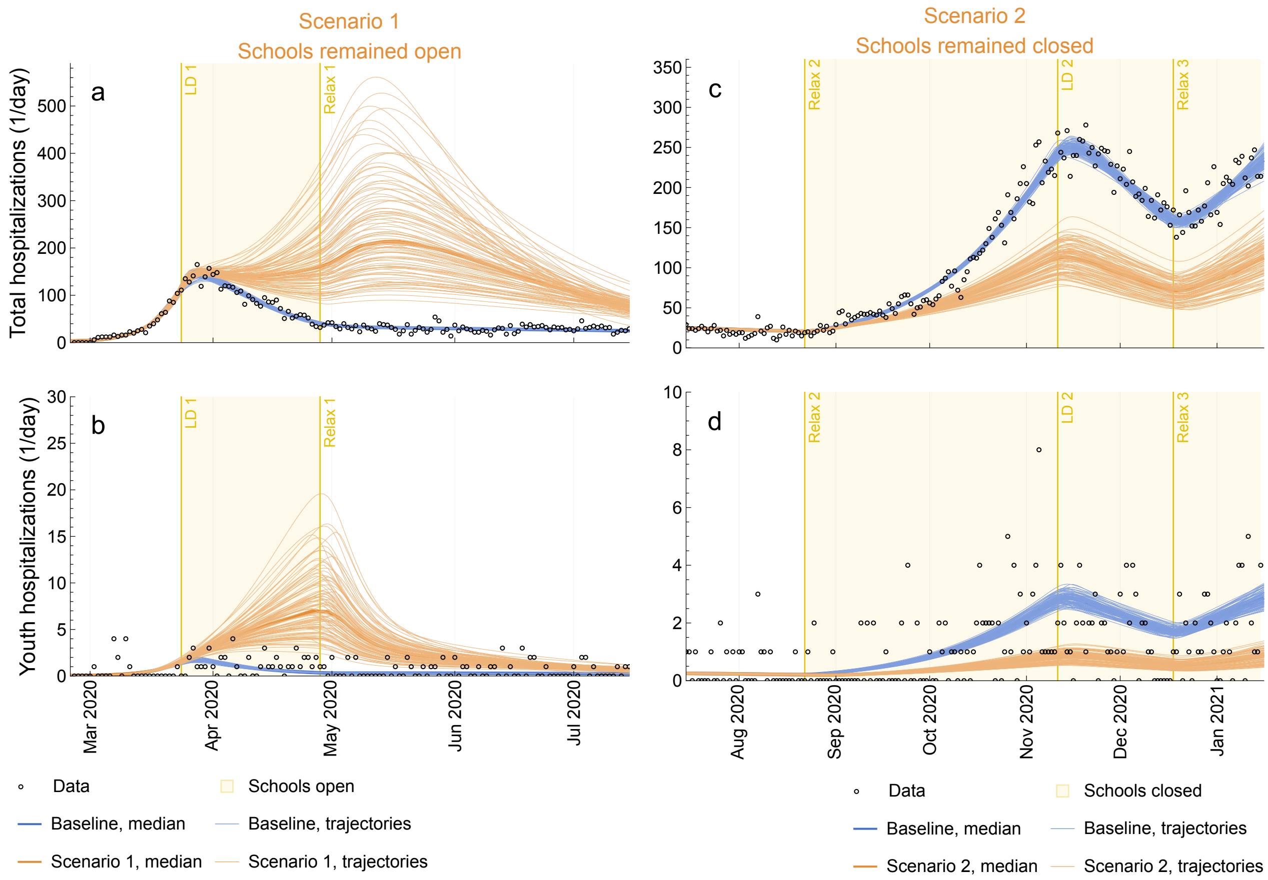

Supplementary Figure 19. Uncertainty in the model projections. Absolute number of (**a**, **c**) total and (**b**, **d**) youth (0-20 years) daily hospital admissions with COVID-19. (**a**, **b**) Scenario 1: schools remained open instead of closing during the first lockdown in spring 2020. (**c**, **d**) Scenario 2: Schools remained closed instead of reopening after the 2020 summer holidays. The circles denote daily hospital admission data. The blue lines are the 100 individual trajectories estimated from the model and the orange lines are the 100 individual trajectories of the respective quantities for Scenarios 1 and 2. Note that, for clarity, we show solutions of the ordinary differential equations without applying the observation model. The yellow-shaded area represents the period when schools were open (**a**, **b**) and closed (**c**, **d**) in the scenario analyses 1 and 2, respectively. LD: lockdown. Relax: relaxation of measures.

Supplementary Section 14 Sensitivity analysis on partial school mitigation levels

In the main analysis, Scenario 1 assumes that schools remained completely open, with pre-pandemic levels of school contacts, while Scenario 2 assumes that schools were completely closed. To explore intermediate situations, we introduced an additional mitigation scaling factor, ξ, applied to the pre-pandemic school contact matrix s_{kl}, as described in Equation (12) for Scenario 1,

$$c_{kl}(t) = [1 - f_0(t)] \underbrace{b_{kl}}_{\substack{\text{pre-pandemic period}\\ \text{school + non-school}\\ \text{contacts}}} + f_0(t)[1 - f_1(t)] \underbrace{[\zeta a_{kl} + \xi s_{kl}]}_{\substack{\text{first lockdown}\\ \text{school + non-school}\\ \text{contacts}}} + f_1(t)[1 - f_2(t)] \underbrace{[u_1 b_{kl} + (1 - u_1)\zeta a_{kl}]}_{\substack{\text{relaxation after first lockdown}\\ \text{school + non-school contacts}}}, \tag{12}$$

and Equation (13) for Scenario 2,

$$\begin{aligned} c_{kl}(t) &= f_1(t)[1 - f_2(t)] \underbrace{[u_1 b_{kl} + (1 - u_1)\zeta a_{kl}]}_{\substack{\text{relaxation after first lockdown}\\ \text{school + non-school contacts}}} + f_2(t)[1 - f_3(t)] \underbrace{[u_2 (b_{kl} - \xi s_{kl}) + (1 - u_2)\zeta a_{kl}]}_{\substack{\text{further relaxation}\\ \text{non-school contacts only}\\ \text{schools closed after summer holidays}}} \\ &+ f_3(t)[1 - f_4(t)] \underbrace{[u_3 (b_{kl} - \xi s_{kl}) + (1 - u_3)\zeta a_{kl}]}_{\substack{\text{second lockdown}\\ \text{non-school contacts}}} + f_4(t) \underbrace{[u_4 (b_{kl} - \xi s_{kl}) + (1 - u_4)\zeta a_{kl}]}_{\substack{\text{relaxation after second lockdown}\\ \text{non-school contacts}}}. \end{aligned} \tag{13}$$

The parameter ξ varies from 0 to 1 in increments of 0.1, allowing us to simulate different levels of school mitigation. For each scenario, $\xi = 0$ reproduces the corresponding baseline (Equations (2) and (4)), while $\xi = 1$ reproduces the scenario under consideration (Equations (3) and (5)). Intermediate values represent partial school openings or closures. Results on select model outcomes are in Figure 4 and in Supplementary Figure 20.

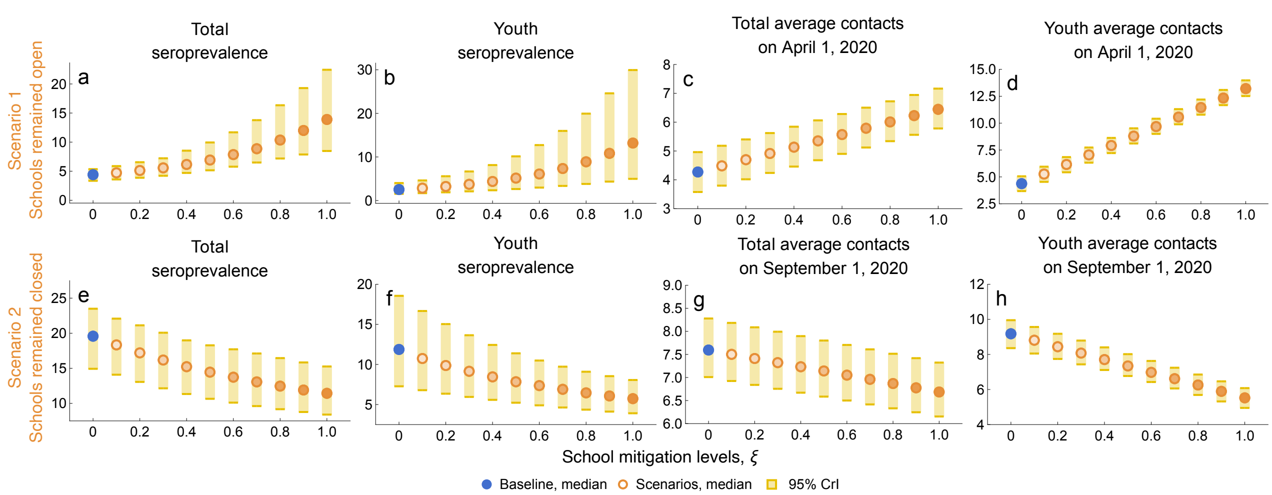

Supplementary Figure 20. Impact of varying school measure mitigation levels on seroprevalence and average contacts. Results for (**a**, **b**, **c**, **d**) Scenario 1: schools remained open instead of closing during the first lockdown in spring 2020 and (**e**, **f**, **g**, **h**) Scenario 2: schools remained closed instead of reopening after the 2020 summer holidays. In particular, shown are respective (**a**, **e**) total and (**b**, **f**) youth seroprevalence, and (**c**, **g**) total and (**d**, **h**) youth average contacts on the onset of the counterfactual scenarios (1 April 2020 for Scenario 1 and 1 September 2020 for Scenario 2). The blue marker ($\xi = 0$) pertains to the median values estimated from the model reflecting the baseline or real-world scenario. The solid orange marker ($\xi = 1$) pertains to the respective median values for counterfactual Scenarios 1 and 2. The markers with increasing orange opacity ($\xi = 0.1, \ldots, 0.9$) pertains to school measure mitigation levels applied to Scenario 1 and 2. The yellow-shaded region correspond to the 95% CrI of the posterior predictive distributions (based on $n = 100$ independent model runs).

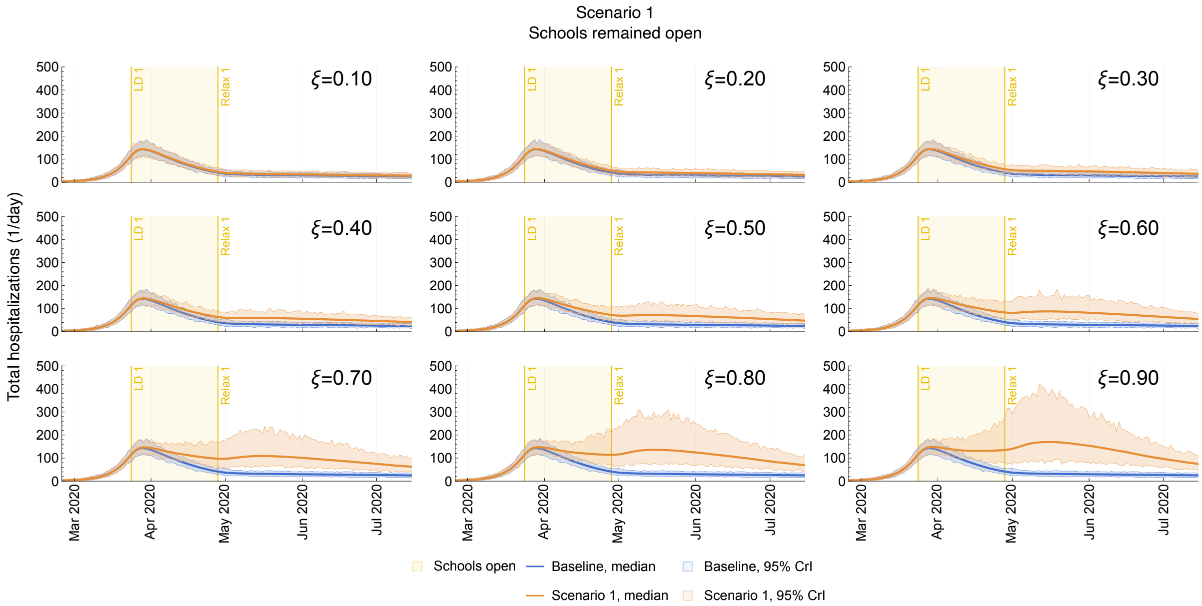

Supplementary Figure 21. Impact of partial openings on total hospitalizations. Absolute number of total daily hospital admissions with COVID-19. Each panel corresponds to a different value of the mitigation factor ξ, which is applied to the pre-pandemic school contact matrix to simulate different levels of school mitigation. The blue lines are the median trajectories estimated from the model reflecting the baseline scenario and the blue-shaded regions correspond to the 95% CrI of the posterior predictive distribution. The orange lines and the orange-shaded regions are the respective quantities for Scenario 1. The yellow-shaded area represents the period when schools were open in the counterfactual scenario analyses. LD: lockdown. Relax: relaxation of measures.

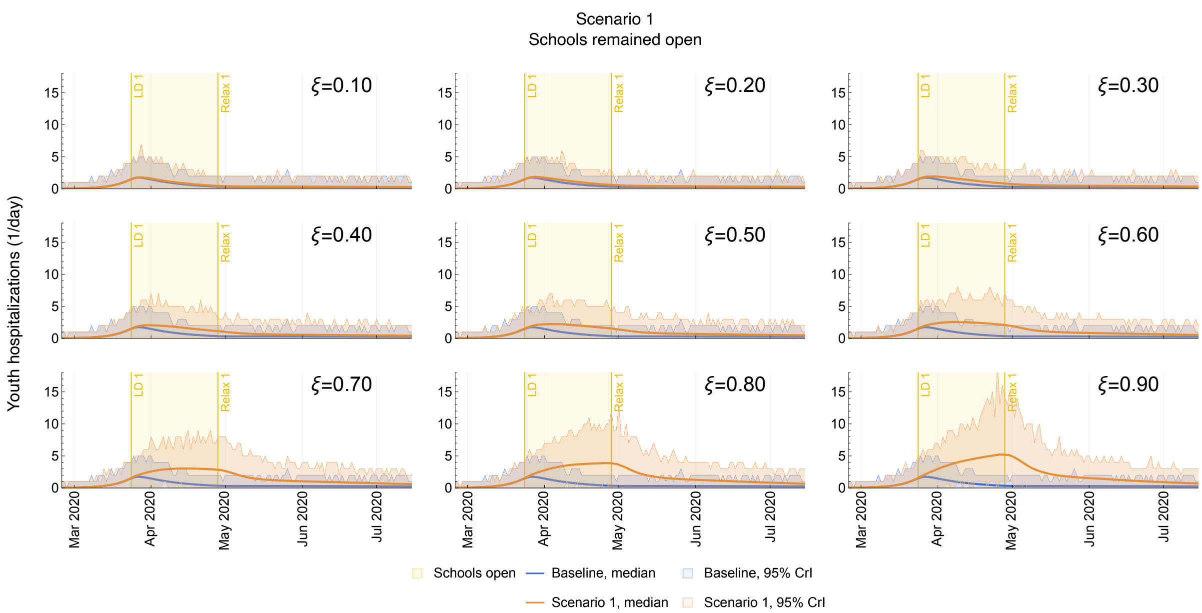

Supplementary Figure 22. Impact of partial openings on youth hospitalizations. Absolute number of youth (0-20 years) daily hospital admissions with COVID-19. Each panel corresponds to a different value of the mitigation factor ξ, which is applied to the pre-pandemic school contact matrix to simulate different levels of school mitigation. The blue lines are the median trajectories estimated from the model reflecting the baseline scenario and the blue-shaded regions correspond to the 95% CrI of the posterior predictive distribution. The orange lines and the orange-shaded regions are the respective quantities for Scenario 1. The yellow-shaded area represents the period when schools were open in the counterfactual scenario analyses. LD: lockdown. Relax: relaxation of measures.

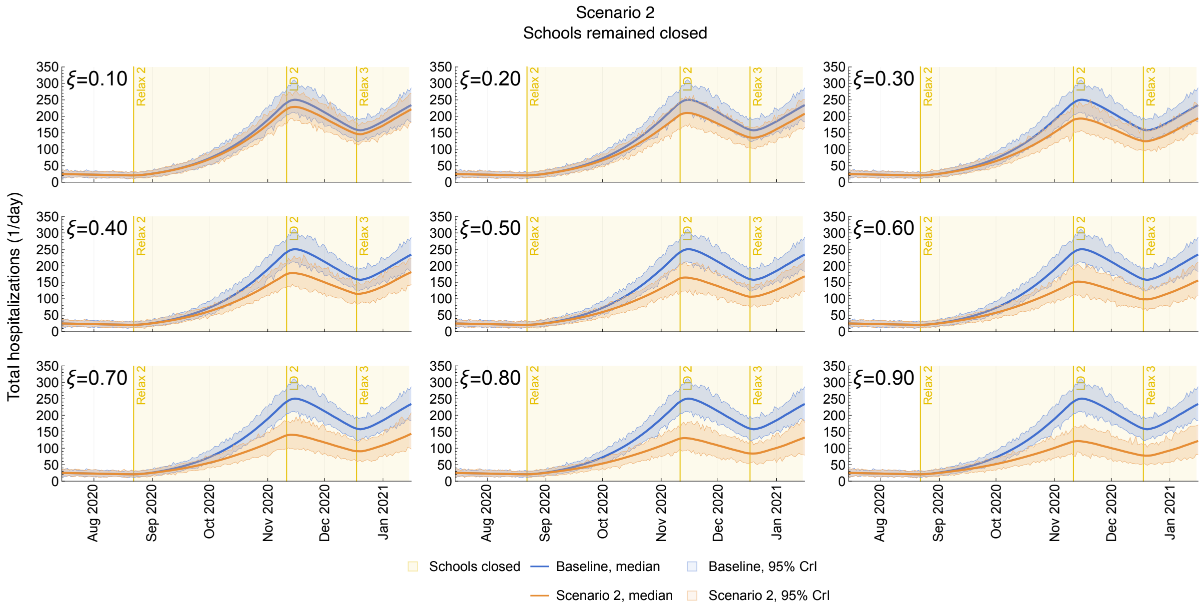

Supplementary Figure 23. Impact of partial closures on total hospitalizations. Absolute number of total daily hospital admissions with COVID-19. Each panel corresponds to a different value of the mitigation factor ξ, which is applied to the pre-pandemic school contact matrix to simulate different levels of school mitigation. The blue lines are the median trajectories estimated from the model reflecting the baseline scenario and the blue-shaded regions correspond to the 95% CrI of the posterior predictive distribution. The orange lines and the orange-shaded regions are the respective quantities for Scenario 2. The yellow-shaded area represents the period when schools were closed in the counterfactual scenario analyses. LD: lockdown. Relax: relaxation of measures.

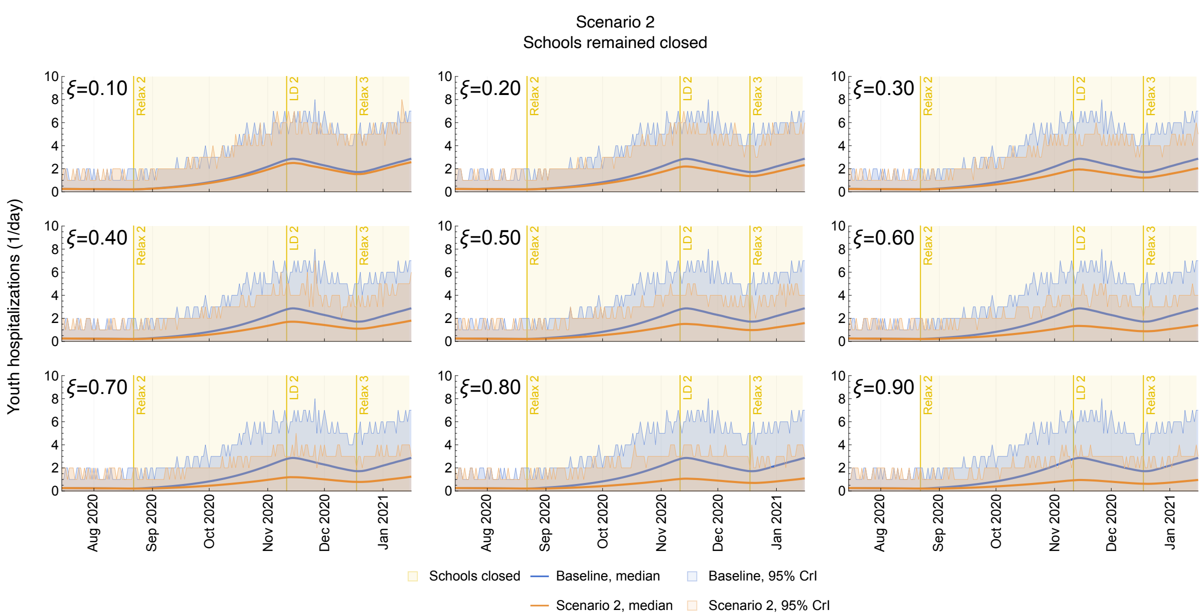

Supplementary Figure 24. Impact of partial closures on youth hospitalizations. Absolute number of youth (0-20 years) daily hospital admissions with COVID-19. Each panel corresponds to a different value of the mitigation factor ξ, which is applied to the pre-pandemic school contact matrix to simulate different levels of school mitigation. The blue lines are the median trajectories estimated from the model reflecting the baseline scenario and the blue-shaded regions correspond to the 95% CrI of the posterior predictive distribution. The orange lines and the orange-shaded regions are the respective quantities for Scenario 2. The yellow-shaded area represents the period when schools were closed in the counterfactual scenario analyses. LD: lockdown. Relax: relaxation of measures.

Summary

Supplementary Table 6. Summary of results for varying school mitigation levels in Scenario 1. This table provides an overview of selected model outcomes for sensitivity analyses of Scenario 1. Most quantities are obtained at the end date (July 15, 2020), and specific date in the counterfactual period of interest (April 1, 2020). Peak values and dates are obtained across all samples.

Model outcomes	**Scenarios**					
	Baseline ($\xi = 0$)	$\xi = 0.10$	$\xi = 0.20$	$\xi = 0.30$	$\xi = 0.40$	$\xi = 0.50$
Hospitalizations						
Total, cumu.	6452 (6161 – 6706)	6868 (6629 – 7179)	7329 (6895 – 7810)	7965 (7432 – 9075)	8741 (7805 – 10443)	9643 (8153 – 12461)
Total, peak val.	143 (126 – 169)	144 (127 – 170)	144 (129 – 171)	145 (123 – 173)	145 (129 – 170)	146 (129 – 173)
Total, peak date	Mar 29 (Mar 25 – Apr 02)	Mar 29 (Mar 24 – Apr 03)	Mar 29 (Mar 25 – Apr 04)	Mar 29 (Mar 24 – Apr 02)	Mar 29 (Mar 24 – Apr 06)	Mar 29 (Mar 24 – Apr 05)
Youth, cumu.	68 (46 – 81)	76 (56 – 94)	87 (68 – 106)	102 (79 – 133)	118 (80 – 156)	139 (98 – 200)
Youth, peak val.	2 (1 – 4)	2 (1 – 5)	2 (1 – 5)	2 (0 – 4)	2 (1 – 5)	2 (0 – 5)
Youth, peak date	Mar 27 (Mar 16 – May 08)	Mar 28 (Mar 15 – Jun 13)	Mar 28 (Mar 17 – Jun 02)	Mar 29 (Mar 15 – Jun 22)	Mar 31 (Mar 15 – May 08)	Apr 03 (Mar 18 – Jun 03)
Seroprevalence						
Total, end	4.40 (3.35 – 5.35)	4.71 (3.58 – 5.87)	5.12 (3.87 – 6.54)	5.57 (4.21 – 7.22)	6.16 (4.70 – 8.53)	6.92 (5.15 – 9.94)
Youth, end	2.52 (1.54 – 4.02)	2.84 (1.70 – 4.61)	3.23 (1.88 – 5.58)	3.72 (2.11 – 6.68)	4.37 (2.36 – 8.14)	5.15 (2.64 – 10.14)
Contacts						
Total, Apr 1	4.27 (3.58 – 4.96)	4.49 (3.80 – 5.18)	4.70 (4.02 – 5.40)	4.91 (4.24 – 5.62)	5.13 (4.46 – 5.84)	5.35 (4.68 – 6.06)
Youth, Apr 1	4.37 (3.68 – 5.06)	5.26 (4.54 – 5.95)	6.16 (5.43 – 6.84)	7.05 (6.32 – 7.73)	7.92 (7.22 – 8.63)	8.79 (8.11 – 9.52)
Reproduction number and cumulative elasticities						
$\mathcal{R}(t)$, Apr 1	0.71 (0.65 – 0.78)	0.74 (0.68 – 0.81)	0.76 (0.70 – 0.84)	0.80 (0.72 – 0.88)	0.84 (0.76 – 0.93)	0.88 (0.79 – 0.98)
$e_k(t)$, Apr 1	0.10 (0.06 – 0.15)	0.13 (0.07 – 0.21)	0.18 (0.09 – 0.28)	0.23 (0.12 – 0.38)	0.30 (0.14 – 0.48)	0.37 (0.18 – 0.58)

	$\xi = 0.60$	$\xi = 0.70$	$\xi = 0.80$	$\xi = 0.90$	Scenario 1 ($\xi = 1$)
Hospitalizations					
Total, cumu.	10783 (8740 – 14847)	12184 (9442 – 18258)	13888 (10109 – 21886)	15935 (11212 – 26299)	18283 (12379 – 31854)
Total, peak val.	147 (128 – 180)	149 (132 – 221)	153 (125 – 290)	170 (124 – 409)	213 (120 – 563)
Total, peak date	Mar 29 (Mar 23 – May 17)	Mar 30 (Mar 24 – May 28)	Mar 30 (Mar 03 – May 05)	May 14 (Mar 26 – May 30)	May 14 (Mar 27 – May 26)
Youth, cumu.	166 (117 – 247)	199 (129 – 300)	241 (135 – 394)	293 (165 – 508)	355 (200 – 624)
Youth, peak val.	3 (1 – 7)	3 (1 – 8)	4 (0 – 12)	5 (1 – 14)	7 (2 – 19)
Youth, peak date	Apr 08 (Mar 17 – Apr 25)	Apr 15 (Mar 20 – May 03)	Apr 26 (Apr 04 – May 12)	Apr 28 (Apr 06 – May 08)	Apr 28 (Apr 07 – May 09)
Seroprevalence					
Total, end	7.85 (5.77 – 11.68)	8.86 (6.49 – 13.78)	10.35 (7.18 – 16.34)	12.00 (7.87 – 19.29)	13.89 (8.47 – 22.44)
Youth, end	6.09 (2.97 – 12.73)	7.35 (3.35 – 15.98)	8.89 (3.81 – 19.94)	10.83 (4.35 – 24.61)	13.19 (4.98 – 29.95)
Contacts					
Total, Sep 1	5.57 (4.90 – 6.28)	5.79 (5.12 – 6.50)	6.01 (5.34 – 6.72)	6.23 (5.56 – 6.94)	6.44 (5.78 – 7.16)
Youth, Sep 1	9.68 (9.00 – 10.41)	10.56 (9.89 – 11.30)	11.45 (10.79 – 12.19)	12.33 (11.67 – 13.08)	13.21 (12.52 – 13.98)
Reproduction number and cumulative elasticities					
$\mathcal{R}(t)$, Sep 1	0.92 (0.83 – 1.06)	0.98 (0.87 – 1.15)	1.04 (0.90 – 1.24)	1.11 (0.94 – 1.34)	1.17 (0.98 – 1.44)
$e_k(t)$, Sep 1	0.45 (0.21 – 0.66)	0.52 (0.25 – 0.72)	0.58 (0.30 – 0.77)	0.64 (0.34 – 0.80)	0.68 (0.39 – 0.83)

Supplementary Table 7. Summary of results for varying school mitigation levels in Scenario 2. This table provides an overview of selected model outcomes for sensitivity analyses of Scenario 2. Most quantities are obtained at the end date (January 15, 2020), and specific date in the counterfactual period of interest (September 1, 2020). Peak values and dates are obtained across all samples.

Model outcomes	Scenarios: Baseline ($\xi = 0$)	$\xi = 0.10$	$\xi = 0.20$	$\xi = 0.30$	$\xi = 0.40$	$\xi = 0.50$
Hospitalizations						
Total, cumu.	21507 (20955 – 22075)	20036 (19275 – 20935)	18725 (17457 – 19920)	17531 (15991 – 18836)	16417 (14307 – 18067)	15385 (13180 – 17210)
Total, peak val.*	251 (227 – 286)	229 (212 – 270)	211 (185 – 257)	194 (162 – 240)	178 (146 – 210)	165 (133 – 203)
Total, peak date*	Nov 15 (Nov 08 – Nov 24)	Nov 15 (Nov 07 – Nov 26)	Nov 15 (Nov 07 – Nov 26)	Nov 15 (Nov 06 – Nov 26)	Nov 15 (Nov 07 – Nov 24)	Nov 15 (Nov 04 – Nov 22)
Youth, cumu.	245 (200 – 292)	219 (191 – 261)	196 (153 – 232)	175 (142 – 209)	158 (117 – 199)	143 (102 – 182)
Youth, peak val.*	3 (2 – 6)	3 (2 – 5)	2 (1 – 5)	2 (1 – 4)	2 (0 – 4)	2 (1 – 4)
Youth, peak date*	Nov 14 (Oct 12 – Dec 07)	Nov 14 (Oct 22 – Dec 07)	Nov 14 (Oct 20 – Dec 08)	Nov 14 (Oct 17 – Dec 04)	Nov 14 (Oct 14 – Dec 06)	Nov 14 (Oct 08 – Dec 08)
Seroprevalence						
Total, end	19.57 (14.93 – 23.49)	18.33 (14.08 – 22.08)	17.20 (13.06 – 21.12)	16.17 (12.15 – 20.07)	15.23 (11.33 – 18.98)	14.45 (10.65 – 18.27)
Youth, end	11.87 (7.27 – 18.56)	10.74 (6.79 – 16.67)	9.87 (6.35 – 15.03)	9.14 (5.95 – 13.64)	8.45 (5.58 – 12.43)	7.84 (5.22 – 11.39)
Contacts						
Total, Sep 1	7.59 (7.01 – 8.28)	7.50 (6.92 – 8.18)	7.41 (6.84 – 8.09)	7.32 (6.75 – 7.99)	7.23 (6.67 – 7.90)	7.14 (6.59 – 7.80)
Youth, Sep 1	9.18 (8.36 – 9.95)	8.81 (8.05 – 9.56)	8.44 (7.74 – 9.18)	8.08 (7.43 – 8.79)	7.71 (7.11 – 8.40)	7.34 (6.77 – 8.02)
Reproduction number and cumulative elasticities						
$\mathcal{R}(t)$, Sep 1	1.24 (1.20 – 1.28)	1.23 (1.20 – 1.27)	1.22 (1.19 – 1.26)	1.21 (1.18 – 1.26)	1.20 (1.17 – 1.25)	1.19 (1.16 – 1.24)
$e_k(t)$, Sep 1	0.13 (0.07 – 0.21)	0.12 (0.07 – 0.20)	0.11 (0.07 – 0.18)	0.11 (0.06 – 0.17)	0.10 (0.06 – 0.15)	0.09 (0.06 – 0.14)

Model outcomes	$\xi = 0.60$	$\xi = 0.70$	$\xi = 0.80$	$\xi = 0.90$	Scenario 1 $\xi = 1$
Hospitalizations					
Total, cumu.	14425 (12054 – 16347)	13546 (11014 – 15523)	12749 (10271 – 14934)	12017 (9286 – 14414)	11336 (8742 – 13742)
Total, peak val.*	152 (113 – 193)	141 (103 – 185)	131 (97 – 182)	122 (88 – 154)	114 (74 – 145)
Total, peak date*	Nov 14 (Nov 06 – Nov 23)	Nov 14 (Nov 04 – Nov 23)	Nov 14 (Nov 04 – Nov 27)	Nov 14 (Nov 02 – Nov 27)	Nov 14 (Nov 03 – Nov 27)
Youth, cumu.	129 (92 – 161)	117 (83 – 152)	106 (76 – 142)	96 (66 – 126)	88 (56 – 122)
Youth, peak val.*	1 (0 – 3)	1 (0 – 2)	1 (0 – 3)	1 (0 – 3)	1 (0 – 3)
Youth, peak date*	Nov 15 (Oct 01 – Dec 03)	Nov 15 (Sep 29 – Dec 04)	Nov 15 (Sep 29 – Dec 08)	Nov 15 (Aug 02 – Dec 06)	Nov 15 (Sep 18 – Dec 06)
Seroprevalence					
Total, end	13.73 (10.10 – 17.71)	13.06 (9.61 – 17.11)	12.46 (9.17 – 16.45)	11.90 (8.77 – 15.84)	11.43 (8.40 – 15.26)
Youth, end	7.36 (4.90 – 10.49)	6.90 (4.63 – 9.72)	6.46 (4.36 – 9.09)	6.07 (4.12 – 8.54)	5.73 (3.91 – 8.06)
Contacts					
Total, Sep 1	7.05 (6.50 – 7.71)	6.96 (6.42 – 7.61)	6.87 (6.33 – 7.51)	6.78 (6.25 – 7.42)	6.69 (6.15 – 7.32)
Youth, Sep 1	6.98 (6.43 – 7.63)	6.62 (6.06 – 7.24)	6.26 (5.69 – 6.85)	5.89 (5.32 – 6.47)	5.52 (4.95 – 6.08)
Reproduction number and cumulative elasticities					
$\mathcal{R}(t)$, Sep 1	1.18 (1.15 – 1.23)	1.17 (1.14 – 1.23)	1.17 (1.13 – 1.22)	1.16 (1.12 – 1.21)	1.15 (1.11 – 1.21)
$e_k(t)$, Sep 1	0.09 (0.05 – 0.13)	0.08 (0.05 – 0.12)	0.07 (0.05 – 0.11)	0.07 (0.04 – 0.10)	0.06 (0.04 – 0.09)

Notes:
*Obtaining peak values and dates are filtered to only capture the uptick in LD 2, i.e., disregarded the last 30 days of the period.

Supplementary Section 15 Sensitivity analyses on fitting seroprevalence to various sampling dates

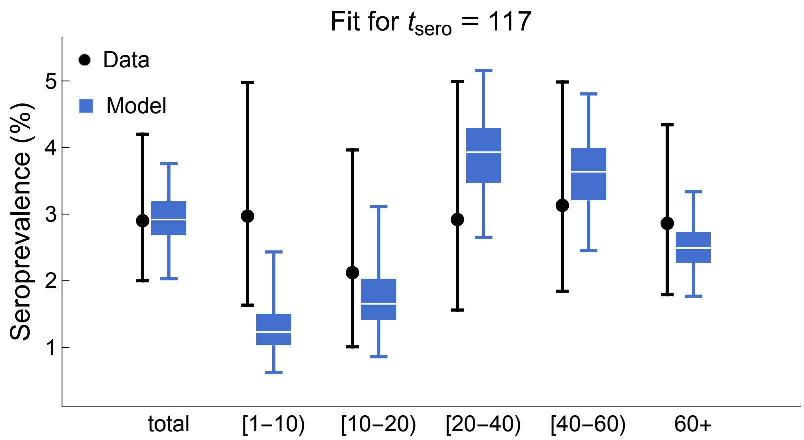

Supplementary Figure 25. Model fit to COVID-19 seroprevalence if $t_{\mathbf{sero}} = 117$. Both total and age-specific seroprevalence are shown in the plot. The black circles with 95% confidence intervals represent the data obtained from the first serological survey (ISNCOVID-19) conducted in Portugal between 21 May 2020 and 8 July 2020 [64] used for fitting the model. The blue box plots represent the marginal posterior distribution of the seroprevalence as the fitting date is adjusted to 21 June 2020, based on 2000 samples from the joint posterior parameter distribution.

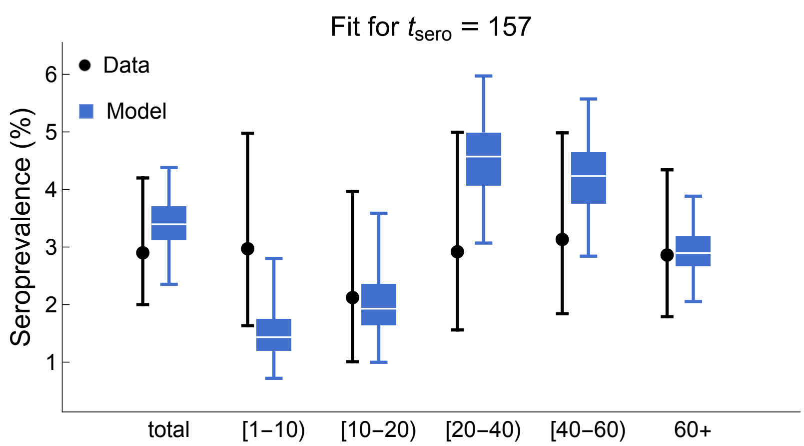

Supplementary Figure 26. Model fit to COVID-19 seroprevalence if $t_{\mathbf{sero}} = 157$. Both total and age-specific seroprevalence are shown in the plot. The black circles with 95% confidence intervals represent the data obtained from the first serological survey (ISNCOVID-19) conducted in Portugal between 21 May 2020 and 8 July 2020 [64] used for fitting the model. The blue box plots represent the marginal posterior distribution of the seroprevalence as the fitting date is adjusted to 31 July 2020, based on 2000 samples from the joint posterior parameter distribution.

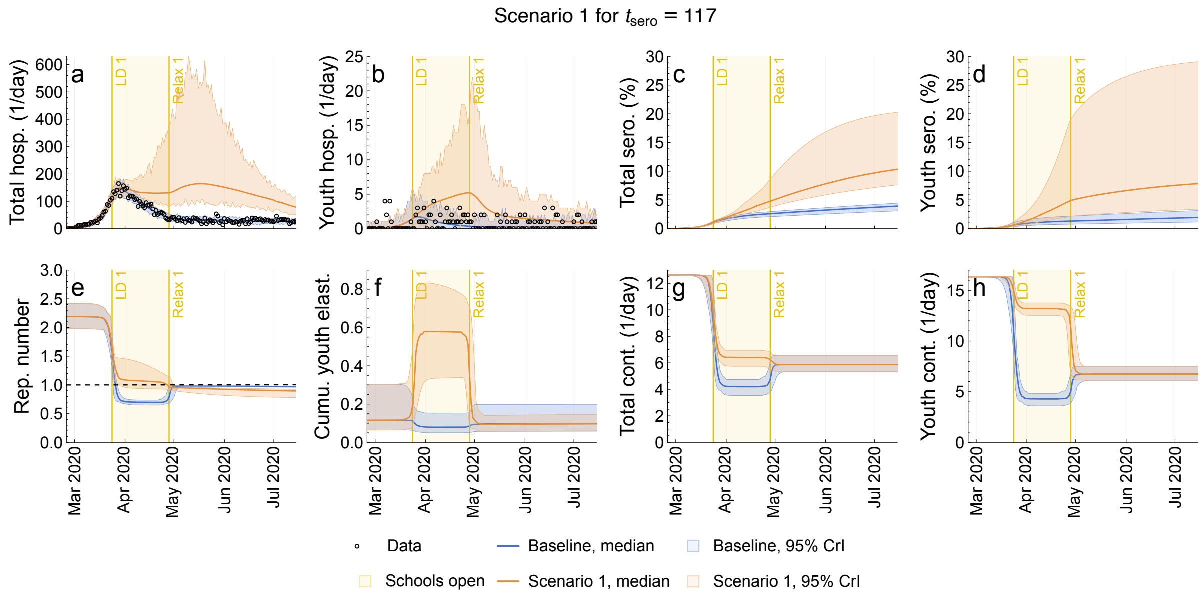

Supplementary Figure 27. Impact of fitting on $t_{\mathbf{sero}} = 117$ on model outcome measures in Scenario 1. Absolute number of (**a**) total and (**b**) youth hospitalizations, (**c**) time-varying reproduction number, and (**d**) relative contribution of youth to $\mathcal{R}(t)$ if seroprevalence fitting date is adjusted to 21 June 2020. The circles denote daily hospital admission data. The dashed line corresponds to $\mathcal{R}(t) = 1$. The blue lines are the median trajectories estimated from the model and the blue-shaded regions correspond to the 95% CrI of the posterior predictive distribution. The orange lines and the orange-shaded regions are the quantities for Scenario 1. The yellow-shaded area represents the period when schools were open in the scenario analysis. LD: lockdown. Relax: relaxation of measures.

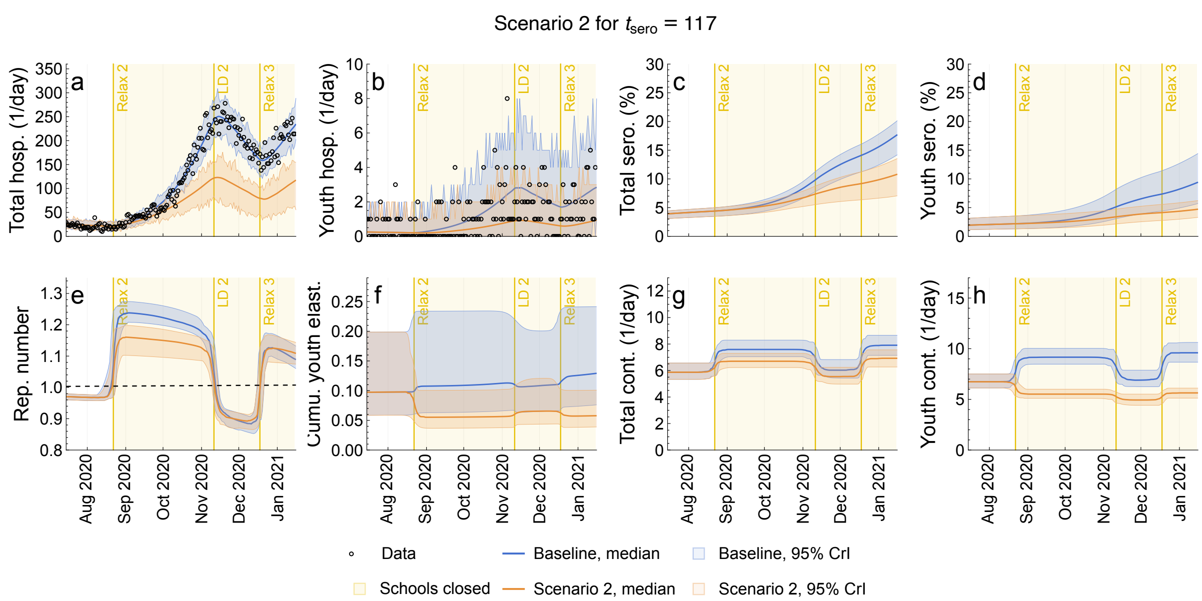

Supplementary Figure 28. Impact of fitting on $t_{\mathbf{sero}} = 117$ on model outcome measures in Scenario 2. Absolute number of (**a**) total and (**b**) youth hospitalizations, (**c**) time-varying reproduction number, and (**d**) relative contribution of youth to $\mathcal{R}(t)$ if seroprevalence fitting date is adjusted to 21 June 2020. The circles denote daily hospital admission data. The dashed line corresponds to $\mathcal{R}(t) = 1$. The blue lines are the median trajectories estimated from the model and the blue-shaded regions correspond to the 95% CrI of the posterior predictive distribution. The orange lines and the orange-shaded regions are the quantities for Scenario 2. The yellow-shaded area represents the period when schools were open in the scenario analysis. LD: lockdown. Relax: relaxation of measures.

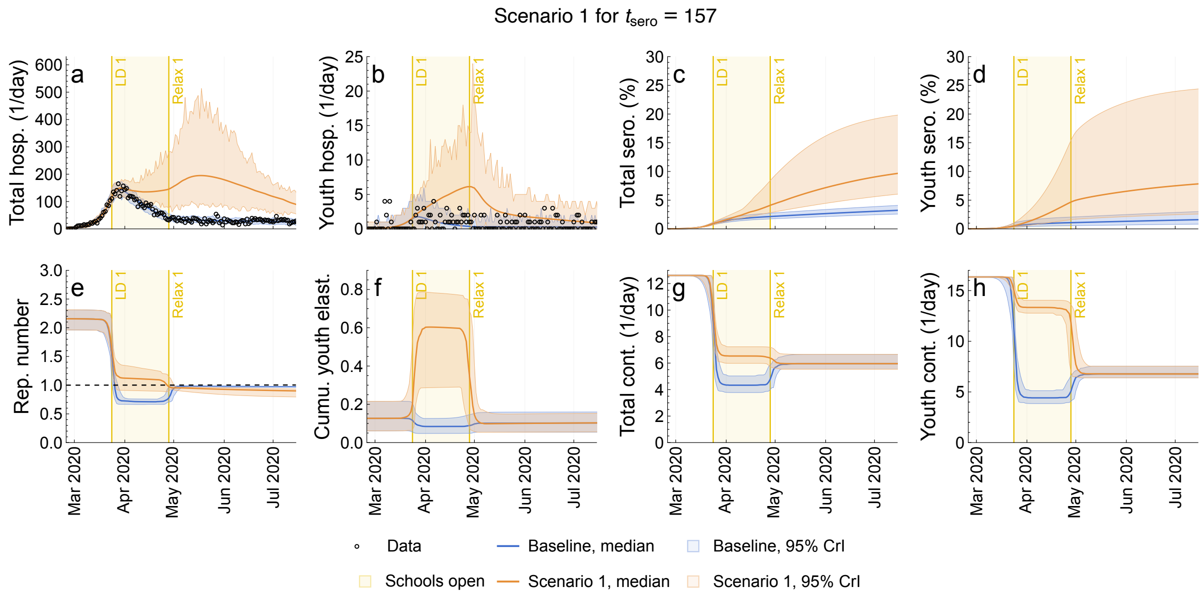

Supplementary Figure 29. Impact of fitting on $t_{\mathbf{sero}} = 157$ on model outcome measures in Scenario 1. Absolute number of (**a**) total and (**b**) youth hospitalizations, (**c**) time-varying reproduction number, and (**d**) relative contribution of youth to $\mathcal{R}(t)$ if seroprevalence fitting date is adjusted to 31 July 2020. The circles denote daily hospital admission data. The dashed line corresponds to $\mathcal{R}(t) = 1$. The blue lines are the median trajectories estimated from the model and the blue-shaded regions correspond to the 95% CrI of the posterior predictive distribution. The orange lines and the orange-shaded regions are the quantities for Scenario 1. The yellow-shaded area represents the period when schools were open in the scenario analysis. LD: lockdown. Relax: relaxation of measures.

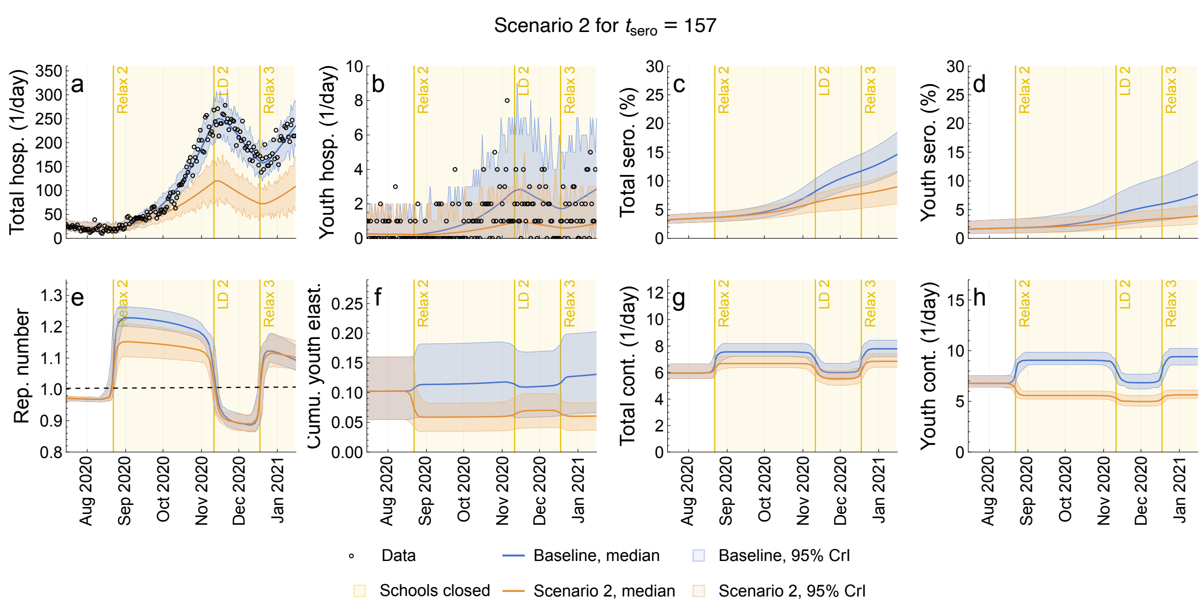

Supplementary Figure 30. Impact of fitting on $t_{\mathbf{sero}} = 157$ on model outcome measures in Scenario 2. Absolute number of (**a**) total and (**b**) youth hospitalizations, (**c**) time-varying reproduction number, and (**d**) relative contribution of youth to $\mathcal{R}(t)$ if seroprevalence fitting date is adjusted to 31 July 2020. The circles denote daily hospital admission data. The dashed line corresponds to $\mathcal{R}(t) = 1$. The blue lines are the median trajectories estimated from the model and the blue-shaded regions correspond to the 95% CrI of the posterior predictive distribution. The orange lines and the orange-shaded regions are the quantities for Scenario 2. The yellow-shaded area represents the period when schools were open in the scenario analysis. LD: lockdown. Relax: relaxation of measures.

Supplementary Table 8. Summary of results for fitting seroprevalence to various sampling dates for Scenario 1. This table provides an overview of selected model outcomes for baseline and Scenario 1. Most quantities are obtained at the end date (July 15, 2020), and specific date in the counterfactual period of interest (April 1, 2020). Peak values and dates are obtained across all samples.

Model outcomes	**Seroprevalence sampling date** $t_{\text{sero}} = 93$	$t_{\text{sero}} = 117$	$t_{\text{sero}} = 157$
Baseline			
Hospitalizations			
Total, cumu.	6452 (6161 – 6706)	6468 (6224 – 6682)	6458 (6190 – 6665)
Total, peak val.	143 (126 – 169)	146 (130 – 170)	145 (122 – 161)
Total, peak date	Mar 29 (Mar 25 – Apr 02)	Mar 28 (Mar 23 – Apr 02)	Mar 28 (Mar 23 – Apr 01)
Youth, cumu.	68 (46 – 81)	68 (45 – 86)	69 (51 – 82)
Youth, peak val.	2 (1 – 4)	2 (1 – 4)	2 (1 – 4)
Youth, peak date	Mar 27 (Mar 16 – May 08)	Mar 27 (Mar 18 – May 18)	Mar 27 (Mar 13 – May 16)
Seroprevalence			
Total, end	4.40 (3.35 – 5.35)	3.90 (3.08 – 4.42)	3.22 (2.58 – 4.07)
Youth, end	2.52 (1.54 – 4.02)	1.94 (1.15 – 3.14)	1.59 (0.83 – 3.00)
Contacts			
Total, Apr 1	4.32 (3.68 – 4.97)	4.25 (3.62 – 4.92)	4.37 (3.81 – 5.13)
Youth, Apr 1	4.48 (3.81 – 5.16)	4.34 (3.71 – 5.05)	4.47 (3.89 – 5.28)
Reproduction number and cumulative elasticities			
$\mathcal{R}(t)$, Apr 1	0.72 (0.65 – 0.80)	0.72 (0.68 – 0.78)	0.73 (0.67 – 0.80)
$e_k(t)$, Apr 1	0.10 (0.06 – 0.15)	0.08 (0.05 – 0.15)	0.08 (0.05 – 0.13)
Scenario 1			
Hospitalizations			
Total, cumu.	18283 (12379 – 31854)	15956 (11745 – 34568)	17935 (11156 – 31018)
Total, peak val.	213 (120 – 563)	165 (124 – 598)	195 (128 – 482)
Total, peak date	May 14 (Mar 27 – May 26)	May 12 (Mar 26 – May 26)	May 14 (Mar 26 – May 29)
Youth, cumu.	355 (200 – 624)	284 (191 – 682)	329 (157 – 634)
Youth, peak val.	7 (2 – 19)	5 (1 – 23)	6 (1 – 19)
Youth, peak date	Apr 28 (Apr 07 – May 09)	Apr 28 (Apr 03 – Jun 08)	Apr 27 (Apr 08 – May 07)
Seroprevalence			
Total, end	13.89 (8.47 – 22.44)	10.30 (7.59 – 20.23)	9.62 (6.01 – 19.78)
Youth, end	13.19 (4.98 – 29.95)	7.82 (3.37 – 29.03)	7.81 (2.57 – 24.34)
Contacts			
Total, Apr 1	6.49 (5.78 – 7.17)	6.44 (5.80 – 6.97)	6.55 (6.00 – 7.33)
Youth, Apr 1	13.23 (12.57 – 13.98)	13.22 (12.56 – 13.76)	13.35 (12.79 – 14.05)
Reproduction number and cumulative elasticities			
$\mathcal{R}(t)$, Apr 1	1.18 (0.99 – 1.45)	1.09 (0.97 – 1.46)	1.12 (0.91 – 1.35)
$e_k(t)$, Apr 1	0.68 (0.37 – 0.83)	0.58 (0.31 – 0.83)	0.60 (0.29 – 0.79)

Supplementary Table 9. Summary of results for fitting seroprevalence to various sampling dates for Scenario 2. This table provides an overview of selected model outcomes for baseline and Scenario 2. Most quantities are obtained at the end date (January 15, 2020), and specific date in the counterfactual period of interest (September 1, 2020). Peak values and dates are obtained across all samples.

Model outcomes	Seroprevalence sampling date		
	$t_{\text{sero}} = 93$	$t_{\text{sero}} = 117$	$t_{\text{sero}} = 157$
Baseline			
Hospitalizations			
Total, cumu.	21507 (20955 – 22075)	21511 (21027 – 21887)	21477 (20959 – 21829)
Total, peak val.*	251 (227 – 286)	251 (232 – 278)	250 (240 – 290)
Total, peak date*	Nov 15 (Nov 08 – Nov 24)	Nov 15 (Nov 09 – Nov 22)	Nov 15 (Nov 10 – Nov 27)
Youth, cumu.	245 (200 – 292)	241 (205 – 300)	243 (216 – 285)
Youth, peak val.*	3 (2 – 6)	3 (2 – 5)	3 (1 – 5)
Youth, peak date*	Nov 14 (Oct 12 – Dec 07)	Nov 14 (Oct 21 – Dec 09)	Nov 14 (Oct 21 – Dec 01)
Seroprevalence			
Total, end	19.57 (14.93 – 23.49)	17.40 (13.93 – 19.81)	14.39 (11.26 – 18.17)
Youth, end	11.87 (7.27 – 18.56)	9.25 (5.60 – 14.18)	7.49 (3.93 – 13.28)
Contacts			
Total, Sep 1	7.59 (7.01 – 8.28)	7.56 (6.99 – 8.29)	7.55 (7.07 – 8.19)
Youth, Sep 1	9.17 (8.36 – 9.95)	9.09 (8.43 – 10.03)	9.06 (8.48 – 9.85)
Reproduction number and cumulative elasticities			
$\mathcal{R}(t)$, Sep 1	1.24 (1.20 – 1.28)	1.24 (1.20 – 1.27)	1.23 (1.20 – 1.26)
$e_k(t)$, Sep 1	0.13 (0.07 – 0.21)	0.11 (0.06 – 0.23)	0.11 (0.06 – 0.18)
Scenario 2			
Hospitalizations			
Total, cumu.	11336 (8742 – 13742)	12248 (7940 – 14162)	11574 (8726 – 14667)
Total, peak val.*	114 (74 – 145)	123 (71 – 157)	120 (82 – 174)
Total, peak date*	Nov 14 (Nov 03 – Nov 27)	Nov 13 (Oct 31 – Nov 24)	Nov 14 (Nov 01 – Nov 21)
Youth, cumu.	88 (56 – 122)	93 (47 – 133)	95 (66 – 129)
Youth, peak val.*	1 (0 – 3)	1 (0 – 2)	1 (0 – 4)
Youth, peak date*	Nov 15 (Sep 18 – Dec 06)	Nov 15 (Oct 22 – Dec 05)	Nov 15 (Oct 20 – Dec 09)
Seroprevalence			
Total, end	11.43 (8.40 – 15.26)	10.67 (6.99 – 13.35)	8.88 (5.96 – 11.50)
Youth, end	5.73 (3.91 – 8.06)	4.67 (3.26 – 6.17)	3.84 (2.49 – 5.65)
Contacts			
Total, Sep 1	6.68 (6.15 – 7.32)	6.68 (6.19 – 7.30)	6.68 (6.31 – 7.25)
Youth, Sep 1	5.54 (4.95 – 6.08)	5.53 (5.11 – 6.01)	5.58 (5.23 – 6.02)
Reproduction number and cumulative elasticities			
$\mathcal{R}(t)$, Sep 1	1.15 (1.11 – 1.21)	1.16 (1.10 – 1.20)	1.15 (1.10 – 1.21)
$e_k(t)$, Sep 1	0.06 (0.04 – 0.09)	0.06 (0.04 – 0.10)	0.06 (0.03 – 0.08)

Notes:
*Obtaining peak values and dates are filtered to only capture the uptick in LD 2, i.e., disregarded the last 30 days of the period.

Supplementary Section 16 Sensitivity analyses for Scenario 1

Scenario 1.1: Strict lockdown across counterfactual period

In the main analyses, Scenario 1 assumes that the strict lockdown affecting non-school contacts, represented by the contact matrix ζa_{kl}, is only contained in the first lockdown regime. In Scenario 1.1, described by Equation (14), we instead assume that the strict lockdown is maintained throughout due to the large wave of hospitalizations resulting from schools remaining open.

$$c_{kl}(t) = [1 - f_0(t)] \underbrace{[b_{kl} - s_{kl}]}_{\substack{\text{pre-pandemic period} \\ \text{non-school contacts}}} + f_0(t)[1 - f_2(t)] \underbrace{\zeta a_{kl}}_{\substack{\text{LD 1} \\ \text{non-school contacts}}} + [1 - f_s(t)] \underbrace{s_{kl}}_{\substack{\text{pre-pandemic period} \\ + \text{ first lockdown} \\ \text{schools open until} \\ \text{summer holidays}}} . \tag{14}$$

In Equation (14), we assumed that (i) the total contact rate in the pre-pandemic period, b_{kl}, was the sum of school contacts, s_{kl}, and non-school contacts, $(b_{kl} - s_{kl})$ [4]; (ii) schools stayed open during the first lockdown and the first relaxation of measures and closed for summer holidays on 10 June 2020 [68]; (iii) since keeping schools open resulted in a hospitalization wave larger than the first pandemic wave, the relaxation of measures affecting non-school contacts was not implemented until hospitalizations declined to the level at which the first lockdown was relaxed. To formulate this, we modeled the school closures for summer holidays using a logistic function $f_s(t) = 1/\left[1 + e^{-K_s(t-t_s)}\right]$, where t_s corresponds to 10 June 2020 (or $t_s = 106$) [68] and, for simplicity, K_s is chosen so that all schools close on the same day (or $K_s = 10$). The results for this scenario are shown in Supplementary Figure 31 wherein it resulted in a hospitalization wave more sustained at the first half of the first relaxation but with a more pronounced decline by the school holidays. The cumulative youth elasticities are also more prominent throughout the wave as compared to Scenario 1.

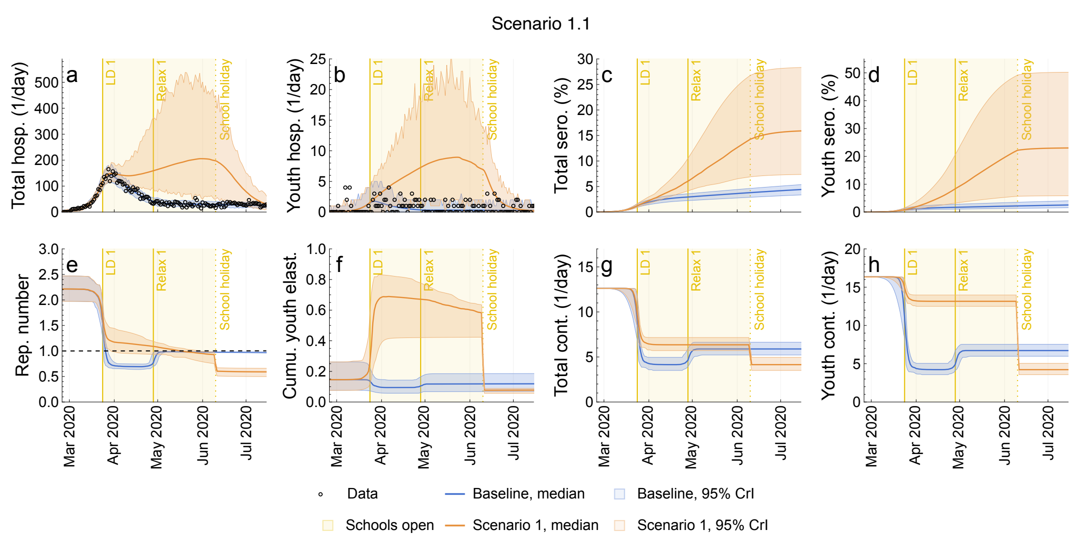

Supplementary Figure 31. Impact of Scenario 1.1 on model outcome measures. Absolute number of (**a**) total and (**b**) youth hospitalizations, (**c**) total and (**d**) youth seroprevalence, (**e**) time-varying reproduction number, (**f**) relative contribution of youth to $\mathcal{R}(t)$, and (**g**) total and (**h**) youth contacts for Scenario 1.1: strict lockdown across counterfactual period. The circles denote daily hospital admission data. The dashed line corresponds to $\mathcal{R}(t) = 1$. The blue lines are the median trajectories estimated from the model and the blue-shaded regions correspond to the 95% CrI of the posterior predictive distribution. The orange lines and the orange-shaded regions are the respective quantities for Scenario 1.1. The yellow-shaded area represents the period when schools were open in the scenario analysis. LD: lockdown. Relax: relaxation of measures.

Scenario 1.2: Extended school opening after lockdown

In the main analyses, Scenario 1 modeled school opening only during the first lockdown period, operating under the hypothesis that the extended first relaxation phase might have already implicitly incorporated some school-related contacts in its later weeks. To explicitly test the impact of school contacts during this relaxation period, Scenario 1.2, defined by Equation (15), extended the school opening using $f_s(t)$ (that is described in Scenario 1.1) to cover both the first lockdown and the first relaxation up until 10 June 2020.

$$c_{kl}(t) = [1 - f_0(t)] \underbrace{[b_{kl} - s_{kl}]}_{\substack{\text{pre-pandemic period}\\ \text{non-school contacts}}} + f_0(t)[1 - f_1(t)] \underbrace{\zeta a_{kl}}_{\substack{\text{LD 1}\\ \text{non-school contacts}}} + f_1(t)[1 - f_2(t)] \underbrace{[u_1 b_{kl} + (1 - u_1)\zeta a_{kl}]}_{\substack{\text{Relax 1}\\ \text{non-school contacts}}} + [1 - f_s(t)] \underbrace{s_{kl}}_{\substack{\text{pre-pandemic period}\\ \text{+ first lockdown}\\ \text{schools open until}\\ \text{summer holidays}}} . \quad (15)$$

As expected, the hospitalization wave in Scenario 1.1 is even larger than in Scenario 1 and in Scenario 1.2. The reproduction number also is above 1 for a longer extent.

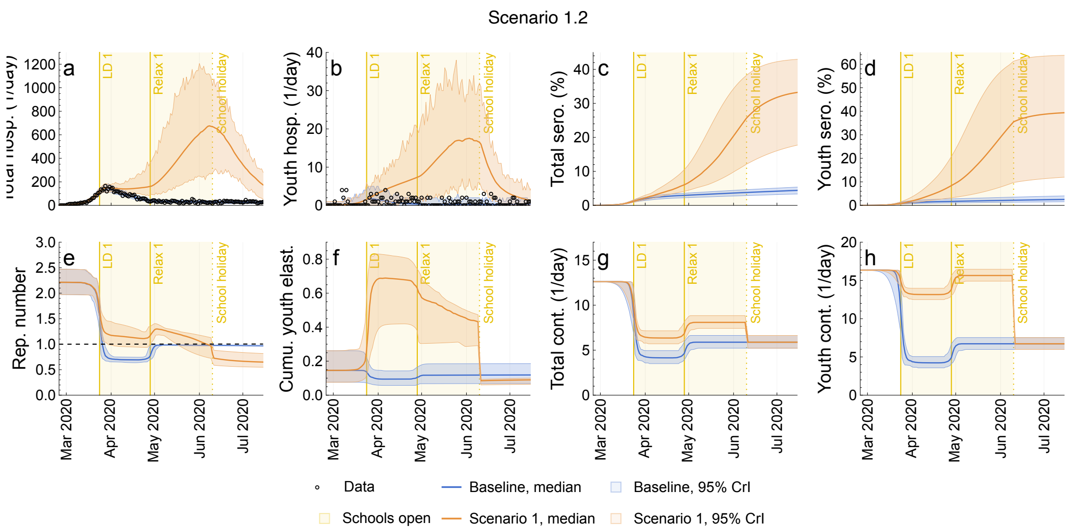

Supplementary Figure 32. Impact of Scenario 1.2 on model outcome measures. Absolute number of (**a**) total and (**b**) youth hospitalizations, (**c**) total and (**d**) youth seroprevalence, (**e**) time-varying reproduction number, (**f**) relative contribution of youth to $\mathcal{R}(t)$, and (**g**) total and (**h**) youth contacts for Scenario 1.2: extending school opening until after the first lockdown. The circles denote daily hospital admission data. The dashed line corresponds to $\mathcal{R}(t) = 1$. The blue lines are the median trajectories estimated from the model and the blue-shaded regions correspond to the 95% CrI of the posterior predictive distribution. The orange lines and the orange-shaded regions are the respective quantities for Scenario 1.1. The yellow-shaded area represents the period when schools were open in the scenario analysis. LD: lockdown. Relax: relaxation of measures.

Summary

Supplementary Table 10. Summary of results for the additional sensitivity analyses for Scenario 1. This table provides an overview of selected model outcomes for baseline and Scenario 1. Most quantities are obtained at the end date (July 15, 2020), and specific date in the counterfactual period of interest (May 1, 2020). Peak values and dates are obtained across all samples.

Model outcomes	**Scenarios**			
	Baseline	Scenario 1	Scenario 1.1	Scenario 1.2
Hospitalizations				
Total, cumu.	6452 (6161 – 6706)	18283 (12379 – 31854)	18027 (9173 – 33136)	40472 (22393 – 60484)
Total, peak val.	143 (126 – 169)	213 (120 – 563)	206 (124 – 548)	695 (283 – 1190)
Total, peak date	Mar 29 (Mar 25 – Apr 02)	May 14 (Mar 27 – May 26)	May 26 (Mar 31 – Jun 14)	Jun 11 (May 24 – Jun 22)
Youth, cumu.	68 (46 – 81)	355 (200 – 624)	613 (246 – 1103)	986 (450 – 1536)
Youth, peak val.	2 (1 – 4)	7 (2 – 19)	9 (1 – 25)	19 (4 – 33)
Youth, peak date	Mar 27 (Mar 16 – May 08)	Apr 28 (Apr 07 – May 09)	May 17 (Apr 24 – Jun 05)	Jun 06 (May 14 – Jun 18)
Seroprevalence				
Total, end	4.40 (3.35 – 5.35)	13.89 (8.47 – 22.44)	15.88 (7.36 – 28.32)	33.16 (17.62 – 42.94)
Youth, end	2.52 (1.54 – 4.02)	13.19 (4.98 – 29.95)	23.01 (5.85 – 50.21)	39.34 (11.93 – 63.75)
Contacts				
Total, May 1	5.49 (4.48 – 6.36)	6.01 (5.26 – 6.87)	6.35 (5.71 – 7.16)	7.69 (6.69 – 8.56)
Youth, May 1	6.15 (4.58 – 7.22)	8.34 (6.44 – 13.35)	13.15 (12.50 – 13.98)	15.07 (13.5 – 16.15)
Reproduction number and cumulative elasticities				
$\mathcal{R}(t)$, May 1	0.92 (0.74 – 0.99)	0.94 (0.90 – 1.06)	1.08 (0.93 – 1.17)	1.25 (1.07 – 1.39)
$e_k(t)$, May 1	0.11 (0.07 – 0.17)	0.18 (0.07 – 0.58)	0.67 (0.42 – 0.77)	0.59 (0.3 – 0.71)

Supplementary Section 17   Sensitivity analyses for Scenario 2

Scenario 2.1: School winter holidays

In the main analyses, Scenario 2 does not account for school closures due to the winter holidays. In Scenario 2.1, defined by Equation (16), we assume that schools are closed during the final period, Relax 3, which begins in mid-December 2020 and coincides with the start of the winter holidays.

$$\begin{aligned} c_{kl}(t) \; = \; & f_1(t)[1-f_2(t)] \underbrace{\left[u_1 b_{kl} + (1-u_1)\zeta a_{kl}\right]}_{\substack{\text{relaxation after first lockdown} \\ \text{school + non-school contacts}}} + f_2(t)[1-f_3(t)] \underbrace{\left[u_2\left(b_{kl}-s_{kl}\right) + (1-u_2)\zeta a_{kl}\right]}_{\substack{\text{further relaxation} \\ \text{non-school contacts only} \\ \text{schools closed after summer holidays}}} \\ + \; & f_3(t)[1-f_4(t)] \underbrace{\left[u_3\left(b_{kl}-s_{kl}\right) + (1-u_3)\zeta a_{kl}\right]}_{\substack{\text{second lockdown} \\ \text{non-school contacts}}} + f_4(t) \underbrace{\left[u_4 b_{kl} + (1-u_4)\zeta a_{kl}\right]}_{\substack{\text{relaxation after second lockdown} \\ \text{non-school contacts}}}. \end{aligned} \tag{16}$$

The results are shown in Supplementary Figure 33. The impact of school holidays on hospitalizations is small.

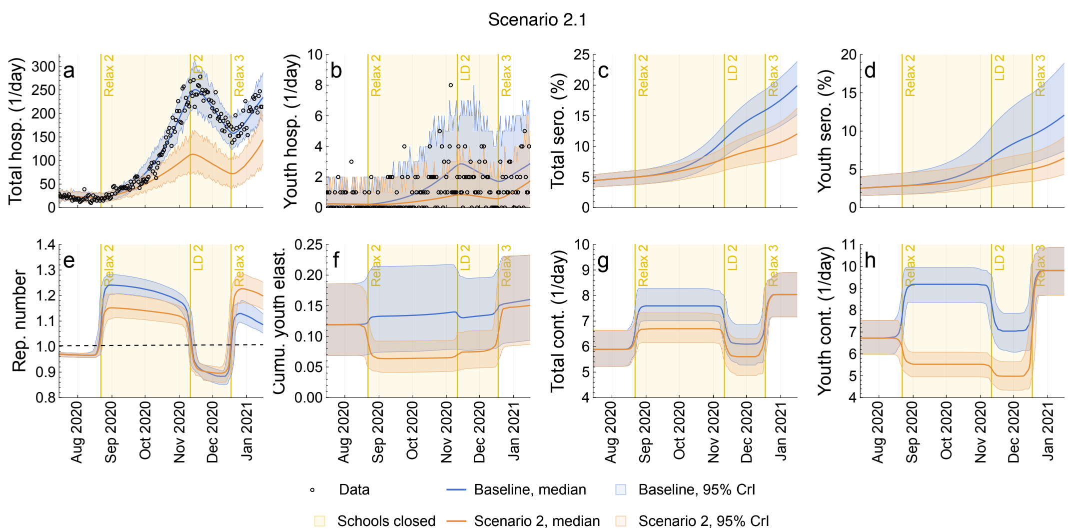

Supplementary Figure 33. Impact of Scenario 2.1 on model outcome measures. Absolute number of (**a**) total and (**b**) youth hospitalizations, (**c**) total and (**d**) youth seroprevalence, (**e**) time-varying reproduction number, (**f**) relative contribution of youth to $\mathcal{R}(t)$, and (**g**) total and (**h**) youth contacts for Scenario 2.1: school winter holidays. The circles denote daily hospital admission data. The dashed line corresponds to $\mathcal{R}(t) = 1$. The blue lines are the median trajectories estimated from the model and the blue-shaded regions correspond to the 95% CrI of the posterior predictive distribution. The orange lines and the orange-shaded regions are the respective quantities for Scenario 2.1. The yellow-shaded area represents the period when schools were closed in the scenario analysis. LD: lockdown. Relax: relaxation of measures.

Scenario 2.2: Alternative reductions in school-based contacts

In the main analyses, the parameters u_j for each period is applied to school contact matrix across all three periods in Scenario 2. This reflects the changing population behavior occurring in within-school measures during the entire Scenario 2 period. In the alternative Scenario 2.2, defined by Equation (17), we instead use a single calibrated parameter ζ_s, representing the mitigation factor in school-based contacts, applied to school contact matrix across all three periods.

$$\begin{aligned} c_{kl}(t) &= f_1(t)[1-f_2(t)]\underbrace{[u_1 b_{kl} + (1-u_1)\zeta a_{kl}]}_{\substack{\text{relaxation after first lockdown}\\ \text{school + non-school contacts}}} + f_2(t)[1-f_3(t)]\underbrace{[u_2 b_{kl} + (1-u_2)\zeta a_{kl} - \zeta_s s_{kl}]}_{\substack{\text{further relaxation}\\ \text{non-school contacts only}\\ \text{schools closed after summer holidays}}} \\ &+ f_3(t)[1-f_4(t)]\underbrace{[u_3 b_{kl} + (1-u_3)\zeta a_{kl} - \zeta_s s_{kl}]}_{\substack{\text{second lockdown}\\ \text{school + non-school contacts}}} + f_4(t)\underbrace{[u_4 b_{kl} + (1-u_4)\zeta a_{kl} - \zeta_s s_{kl}]}_{\substack{\text{relaxation after second lockdown}\\ \text{non-school contacts}}}. \end{aligned} \tag{17}$$

The calibration ensured that non-school contacts did not fall below their level prior to the second relaxation if schools stay closed, i.e.

$$\zeta_s = \min_{k,l}\left\{\underset{x}{\text{argmin}}\ \{[u_2 b_{kl} + (1-u_2)a_{kl} - x s_{kl}] - [u_1 b_{kl} + (1-u_1)a_{kl}]\}\right\}.$$

We ultimately obtained $\zeta_s = 0.18$ (95% CrI $0.16 - 0.20$), lower than all estimated u_j's. The results are shown in Supplementary Figure 34. Compared to Scenario 2 in the main text, this scenario results in a somewhat bigger epidemic wave. However, the overall qualitative behavior of the model remains similar. School closures can mitigate, but not prevent, the autumn 2020 wave.

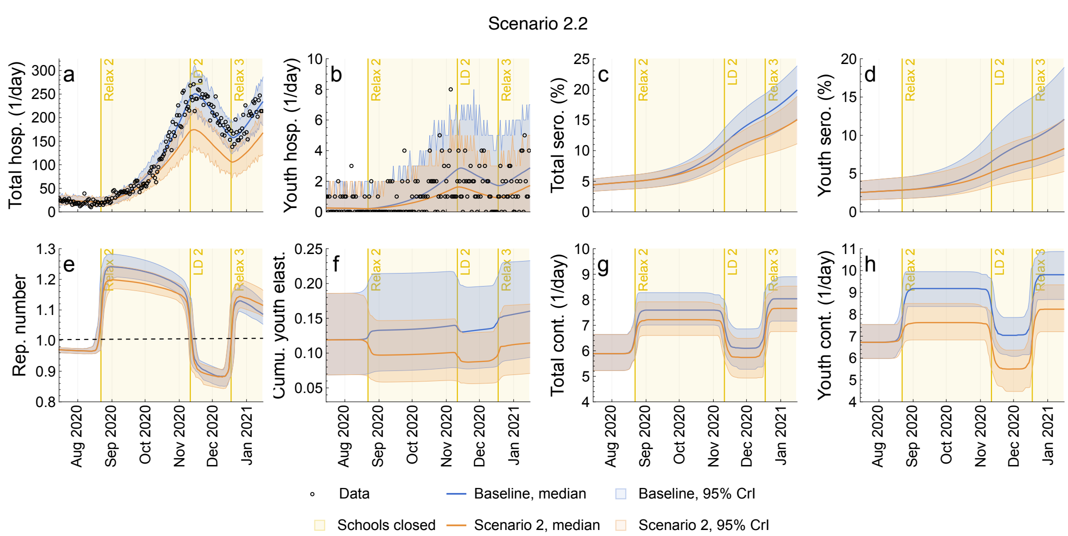

Supplementary Figure 34. Impact of Scenario 2.2 on model outcome measures. Absolute number of (**a**) total and (**b**) youth hospitalizations, (**c**) total and (**d**) youth seroprevalence, (**e**) time-varying reproduction number, (**f**) relative contribution of youth to $\mathcal{R}(t)$, and (**g**) total and (**h**) youth contacts for Scenario 2.2: alternative reductions in school-based contacts. The circles denote daily hospital admission data. The dashed line corresponds to $\mathcal{R}(t) = 1$. The blue lines are the median trajectories estimated from the model and the blue-shaded regions correspond to the 95% CrI of the posterior predictive distribution. The orange lines and the orange-shaded regions are the respective quantities for Scenario 2.2. The yellow-shaded area represents the period when schools were closed in the scenario analysis. LD: lockdown. Relax: relaxation of measures.

Scenario 2.3: Continued Scenario 1

We continue Scenario 1 into the period of Scenario 2 by implementing the same measures as that of the baseline during the second wave. For the contact formulation, Scenario 2.3 basically considered Equation (3) and Equation (4). The results are shown in Figure 35.

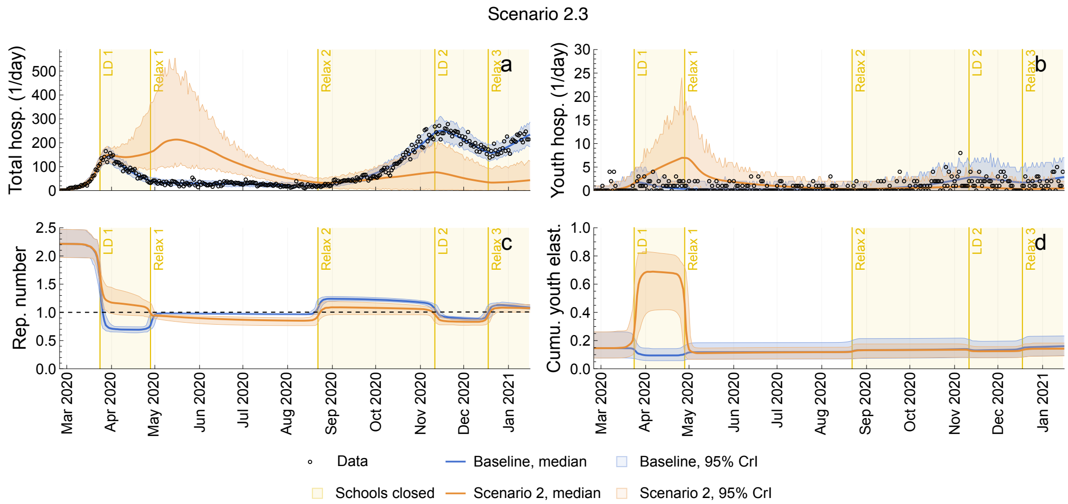

Supplementary Figure 35. Impact of Scenario 2.3 on model outcome measures. Absolute number of (**a**) total and (**b**) youth hospitalizations, (**c**) time-varying reproduction number, and (**d**) relative contribution of youth to $\mathcal{R}(t)$ for Scenario 2.3: continued Scenario 1. The circles denote daily hospital admission data. The dashed line corresponds to $\mathcal{R}(t) = 1$. The blue lines are the median trajectories estimated from the model and the blue-shaded regions correspond to the 95% CrI of the posterior predictive distribution. The orange lines and the orange-shaded regions are the quantities for Scenario 2.3. The yellow-shaded area represents the period when schools were open in the scenario analysis. LD: lockdown. Relax: relaxation of measures.

Summary

Supplementary Table 11. Summary of results for the additional sensitivity analyses for Scenario 2. This table provides an overview of selected model outcomes for baseline and Scenario 2. Most quantities are obtained at the end date (January 15, 2020), and specific date in the counterfactual period of interest (September 1, 2020). Peak values and dates are obtained across all samples.

Model outcomes	Scenarios				
	Baseline	Scenario 2	Scenario 2.1	Scenario 2.2	Scenario 2.3
Hospitalizations					
Total, cumu.	21507 (20955 – 22075)	11336 (8742 – 13742)	17986 (15354 – 20296)	22258 (20272 – 23790)	28650 (25153 – 35579)
Total, peak val.*	251 (227 – 286)	114 (74 – 145)	114 (75 – 148)	175 (139 – 206)	89 (53 – 204)
Total, peak date*	Nov 15 (Nov 08 – Nov 24)	Nov 14 (Nov 05 – Nov 24)	Nov 14 (Nov 03 – Nov 27)	Nov 15 (Nov 06 – Nov 25)	Jul 15 (Jul 07 – Nov 14)
Youth, cumu.	245 (200 – 292)	88 (56 – 122)	166 (135 – 197)	215 (182 – 246)	448 (347 – 658)
Youth, peak val.*	3 (2 – 6)	1 (0 – 3)	1 (0 – 3)	2 (0 – 3)	1 (0 – 4)
Youth, peak date*	Nov 14 (Oct 12 – Dec 07)	Nov 15 (Sep 18 – Dec 06)	Nov 15 (Sep 28 – Dec 07)	Nov 13 (Oct 19 – Dec 05)	Nov 09 (Jul 17 – Dec 11)
Seroprevalence					
Total, end	19.57 (14.93 – 23.49)	11.43 (8.40 – 15.26)	11.83 (8.65 – 15.88)	14.82 (10.97 – 18.53)	20.06 (17.48 – 23.96)
Youth, end	11.87 (7.27 – 18.56)	5.73 (3.91 – 8.06)	6.35 (4.27 – 9.05)	8.14 (5.19 – 11.9)	16.61 (9.24 – 30.57)
Contacts					
Total, Sep 1	7.59 (7.01 – 8.28)	6.68 (6.15 – 7.32)	6.68 (6.15 – 7.32)	7.19 (6.6 – 7.92)	7.59 (7.01 – 8.28)
Youth, Sep 1	9.17 (8.36 – 9.95)	5.54 (4.95 – 6.08)	5.54 (4.95 – 6.08)	7.59 (6.83 – 8.5)	9.17 (8.36 – 9.95)
Reproduction number and cumulative elasticities					
$\mathcal{R}(t)$, Sep 1	1.24 (1.20 – 1.28)	1.15 (1.11 – 1.21)	1.15 (1.11 – 1.21)	1.2 (1.17 – 1.25)	1.09 (0.96 – 1.19)
$e_k(t)$, Sep 1	0.13 (0.07 – 0.21)	0.06 (0.04 – 0.09)	0.06 (0.04 – 0.09)	0.1 (0.06 – 0.15)	0.13 (0.08 – 0.18)

Notes:
*Obtaining peak values and dates are filtered to only capture the uptick in LD 2, i.e., disregarded the last 30 days of the period.

References

[1] Viana, J. *et al.* Controlling the pandemic during the SARS-CoV-2 vaccination rollout. *Nature Communications* **12**, 3674 (2021).

[2] Jing, Q.-L. *et al.* Household secondary attack rate of COVID-19 and associated determinants in Guangzhou, China: a retrospective cohort study. *The Lancet Infectious Diseases* **20**, 1141–1150 (2020).

[3] Viner, R. M. *et al.* Susceptibility to SARS-CoV-2 infection among children and adolescents compared with adults: a systematic review and meta-analysis. *JAMA Pediatrics* **175**, 143–156 (2021).

[4] Mistry, D. *et al.* Inferring high-resolution human mixing patterns for disease modeling. *Nature Communications* **12**, 323 (2021).

[5] PORDATA. Base de Dados Portugal Contemporâneo (2024). URL https://www.pordata.pt/pt.

[6] Backer, J. A. *et al.* Impact of physical distancing measures against COVID-19 on contacts and mixing patterns: repeated cross-sectional surveys, the Netherlands, 2016–17, April 2020 and June 2020. *Eurosurveillance* **26**, 2000994 (2021).

[7] Presidência do Conselho de Ministros. Decreto-Lei n.º 10-A/2020, de 13 de março. Diário da República n.º 52/2020, 1º Suplemento, Série I de 2020-03-13 (2020). URL https://files.diariodarepublica.pt/1s/2020/03/05201/0000200013.pdf. Páginas 22-(2) a 22-(13).

[8] Presidência da República. Decreto do Presidente da República n.º 14-A/2020, de 18 de março. Diário da República n.º 55/2020, 3º Suplemento, Série I de 2020-03-18 (2020). URL https://files.diariodarepublica.pt/1s/2020/03/05503/0000200004.pdf. Páginas 13-(2) a 13-(4).

[9] Presidência do Conselho de Ministros. Decreto n.º 2-A/2020, de 20 de março. Diário da República n.º 57/2020, 1º Suplemento, Série I de 2020-03-20 (2020). URL https://files.diariodarepublica.pt/1s/2020/03/05701/0000500017.pdf. Páginas 11-(5) a 11-(17).

[10] Presidência do Conselho de Ministros. Decreto n.º 2-B/2020, de 2 de abril. Diário da República n.º 66/2020, 2º Suplemento, Série I de 2020-04-02 (2020). URL https://files.diariodarepublica.pt/1s/2020/04/06602/0000200020.pdf. Páginas 31-(2) a 31-(20).

[11] Presidência do Conselho de Ministros. Decreto n.º 2-C/2020, de 17 de abril. Diário da República n.º 76/2020, 1º Suplemento, Série I de 2020-04-17 (2020). URL https://files.diariodarepublica.pt/1s/2020/04/07601/0000900028.pdf. Páginas 7-(9) a 7-(28).

[12] Gabinete do Ministro da Ciência, Tecnologia e Ensino Superior. Recomendação às instituições científicas e de ensino superior relativamente à cessação do estado de emergência motivado pela pandemia COVID-19 (2020). URL /https://wwwcdn.dges.gov.pt/sites/default/files/comunicado_mctes_levantamento_progressivo_v17abr2020_final.pdf.

[13] Presidência do Conselho de Ministros. Resolução do Conselho de Ministros n.º 33-C/2020, de 30 de abril. Diário da República n.º 85/2020, 3º Suplemento, Série I de 2020-04-30 (2020). URL https://files.diariodarepublica.pt/1s/2020/04/08503/0002300025.pdf. Páginas 7-(23) a 7-(25).

[14] Presidência do Conselho de Ministros. Resolução do Conselho de Ministros n.º 33-A/2020, de 30 de abril. Diário da República n.º 85/2020, 3º Suplemento, Série I de 2020-04-30 (2020). URL https://files.diariodarepublica.pt/1s/2020/04/08503/0001000021.pdf. Páginas 7-(10) a 7-(21).

[15] Presidência do Conselho de Ministros. Decreto-Lei n.º 20-H/2020, de 14 de maio. Diário da República n.º 94/2020, 2º Suplemento, Série I de 2020-05-14 (2020). URL https://files.diariodarepublica.pt/1s/2020/05/09402/0000200007.pdf. Páginas 8-(2) a 8-(7).

[16] Presidência do Conselho de Ministros. Resolução do Conselho de Ministros n.º 63-A/2020, de 14 de agosto. Diário da República n.º 158/2020, 1º Suplemento, Série I de 2020-08-14 (2020). URL https://files.diariodarepublica.pt/1s/2020/08/15801/0000200018.pdf. Páginas 138-(2) a 138-(18).

[17] Presidência do Conselho de Ministros. Resolução do Conselho de Ministros n.º 68-A/2020, de 28 de agosto. Diário da República n.º 168/2020, 1º Suplemento, Série I de 2020-08-28 (2020). URL https://files.diariodarepublica.pt/1s/2020/08/16801/0000200002.pdf. Páginas 168-(2) a 168-(2).

[18] Educação - Gabinetes do Secretário de Estado Adjunto e da Educação e da Secretária de Estado da Educação. Despacho n.º 6906-B/2020, de 3 de julho. Diário da República n.º 128/2020, 2º Suplemento, Série II de 2020-07-03 (2020). URL https://files.diariodarepublica.pt/2s/2020/07/128000002/0000400009.pdf. Páginas 360-(4) a 360-(9).

[19] Presidência do Conselho de Ministros. Resolução do Conselho de Ministros n.º 70-A/2020, de 11 de setembro. Diário da República n.º 178/2020, 1º Suplemento, Série I de 2020-09-11 (2020). URL https://files.diariodarepublica.pt/1s/2020/09/17801/0000200015.pdf. Páginas 6-(2) a 6-(15).

[20] Presidência do Conselho de Ministros. Resolução do Conselho de Ministros n.º 88-A/2020, de 14 de outubro. Diário da República n.º 200/2020, 1º Suplemento, Série I de 2020-10-14 (2020). URL https://files.diariodarepublica.pt/1s/2020/10/20001/0000200015.pdf. Páginas 35-(2) a 35-(15).

[21] Presidência do Conselho de Ministros. Resolução do Conselho de Ministros n.º 92-A/2020, de 2 de novembro. Diário da República n.º 213/2020, 1º Suplemento, Série I de 2020-11-02 (2020). URL https://files.diariodarepublica.pt/1s/2020/11/21301/0000200021.pdf. Páginas 11-(2) a 11-(21).

[22] Presidência do Conselho de Ministros. Decreto n.º 8/2020, de 8 de novembro. Diário da República n.º 217-A/2020, Série I de 2020-11-0 (2020). URL https://files.diariodarepublica.pt/1s/2020/11/217a00/0000200008.pdf. Páginas 2 - 8.

[23] Presidência da República. Decreto do Presidente da República n.º 59-A/2020, de 20 de novembro. Diário da República n.º 227/2020, 1º Suplemento, Série I de 2020-11-20 (2020). URL https://files.diariodarepublica.pt/1s/2020/11/22701/0000200004.pdf. Páginas 15-(2) a 15-(4).

[24] Presidência do Conselho de Ministros. Decreto n.º 9/2020, de 21 de novembro. Diário da República n.º 227-A/2020, Série I de 2020-11-21 (2020). URL https://files.diariodarepublica.pt/1s/2020/11/227a00/0000200031.pdf. Páginas 2 - 31.

[25] Presidência da República. Decreto do Presidente da República n.º 61-A/2020, de 4 de dezembro. Diário da República n.º 236/2020, 2º Suplemento, Série I de 2020-12-04 (2020). URL https://files.diariodarepublica.pt/1s/2020/12/23602/0000200004.pdf. Páginas 14-(2) a 14-(4).

[26] Presidência do Conselho de Ministros. Decreto n.º 11/2020, de 6 de dezembro. Diário da República n.º 236-A/2020, Série I de 2020-12-06 (2020). URL https://files.diariodarepublica.pt/1s/2020/12/236a00/0000200033.pdf. Páginas 2 - 33.

[27] Presidência da República. Decreto do Presidente da República n.º 66-A/2020, de 17 de dezembro. Diário da República n.º 244/2020, 1º Suplemento, Série I de 2020-12-17 (2020). URL https://files.diariodarepublica.pt/1s/2020/12/24401/0000200004.pdf. Páginas 21-(2) a 21-(4).

[28] Presidência do Conselho de Ministros. Decreto n.º 11-A/2020, de 21 de dezembro. Diário da República n.º 246/2020, 2º Suplemento, Série I de 2020-12-21 (2020). URL https://files.diariodarepublica.pt/1s/2020/12/24602/0000200040.pdf. Páginas 22-(2) a 22-(40).

[29] Presidência da República. Decreto do Presidente da República n.º 6-A/2021, de 6 de janeiro. Diário da República n.º 3/2021, 1º Suplemento, Série I de 2021-01-06 (2021). URL https://files.diariodarepublica.pt/1s/2021/01/00301/0000200004.pdf. Páginas 38-(2) a 38-(4).

[30] Presidência do Conselho de Ministros. Decreto n.º 2-A/2021, de 7 de janeiro. Diário da República n.º 4/2021, 2º Suplemento, Série I de 2021-01-07 (2021). URL https://files.diariodarepublica.pt/1s/2021/01/00402/0000200040.pdf. Páginas 207-(2) a 207-(40).

[31] Presidência da República. Decreto do Presidente da República n.º 6-B/2021, de 13 de janeiro. Diário da República n.º 8/2021, 2º Suplemento, Série I de 2021-01-13 (2021). URL https://files.diariodarepublica.pt/1s/2021/01/00802/0000200005.pdf. Páginas 5-(2) a 5-(5).

[32] Presidência do Conselho de Ministros. Decreto n.º 3-A/2021, de 14 de janeiro. Diário da República n.º 9/2021, 1º Suplemento, Série I de 2021-01-14 (2021). URL https://files.diariodarepublica.pt/1s/2021/01/00901/0000500029.pdf. Páginas 13-(5) a 13-(29).

[33] Rice, K., Wynne, B., Martin, V. & Ackland, G. J. Effect of school closures on mortality from coronavirus disease 2019: old and new predictions. *BMJ* **371** (2020).

[34] Rozhnova, G. *et al.* Model-based evaluation of school-and non-school-related measures to control the COVID-19 pandemic. *Nature Communications* **12**, 1614 (2021).

[35] Walsh, S. *et al.* Do school closures and school reopenings affect community transmission of COVID-19? A systematic review of observational studies. *BMJ Open* **11**, e053371 (2021).

[36] Littlecott, H. *et al.* Measures implemented in the school setting to contain the COVID-19 pandemic. *The Cochrane Database of Systematic Reviews* **5**, CD015029–CD015029 (2024).

[37] Panovska-Griffiths, J. *et al.* Determining the optimal strategy for reopening schools, the impact of test and trace interventions, and the risk of occurrence of a second COVID-19 epidemic wave in the UK: a modelling study. *The Lancet Child & Adolescent Health* **4**, 817–827 (2020).

[38] Baxter, A., Oruc, B. E., Asplund, J., Keskinocak, P. & Serban, N. Evaluating scenarios for school reopening under COVID19. *BMC Public Health* **22**, 496 (2022).

[39] Ragonnet, R. *et al.* Estimating the impact of school closures on the COVID-19 dynamics in 74 countries: A modelling analysis. *PLOS Medicine* **22**, e1004512 (2025).

[40] Lee, B., Hanley, J. P., Nowak, S., Bates, J. H. & Hébert-Dufresne, L. Modeling the impact of school reopening on SARS-CoV-2 transmission using contact structure data from Shanghai. *BMC Public Health* **20**, 1713 (2020).

[41] Abrams, S. *et al.* Modelling the early phase of the belgian covid-19 epidemic using a stochastic compartmental model and studying its implied future trajectories. *Epidemics* **35**, 100449 (2021).

[42] Dekker, M. M., Coffeng, L. E., Pijpers, F. P., Panja, D. & de Vlas, S. J. Reducing societal impacts of SARS-CoV-2 interventions through subnational implementation. *Elife* **12**, e80819 (2023).

[43] Yuan, P. *et al.* School and community reopening during the COVID-19 pandemic: a mathematical modelling study. *Royal Society Open Science* **9**, 211883 (2022).

[44] Prem, K. *et al.* The effect of control strategies to reduce social mixing on outcomes of the COVID-19 epidemic in Wuhan, China: a modelling study. *The Lancet Public Health* **5**, e261–e270 (2020).

[45] Lasser, J. *et al.* Assessing the impact of SARS-CoV-2 prevention measures in Austrian schools using agent-based simulations and cluster tracing data. *Nature Communications* **13**, 554 (2022).

[46] Leng, T. *et al.* Quantifying pupil-to-pupil SARS-CoV-2 transmission and the impact of lateral flow testing in English secondary schools. *Nature Communications* **13**, 1106 (2022).

[47] Colosi, E., Lina, B., Elias, C., Vanhems, P. & Colizza, V. Proactive vs. reactive covid-19 screening in schools: lessons from experimental protocols in france during the delta and omicron waves. *medRxiv* (2025).

[48] McGee, R. S., Homburger, J. R., Williams, H. E., Bergstrom, C. T. & Zhou, A. Y. Model-driven mitigation measures for reopening schools during the COVID-19 pandemic. *Proceedings of the National Academy of Sciences* **118**, e2108909118 (2021).

[49] Lessler, J. *et al.* Household COVID-19 risk and in-person schooling. *Science* **372**, 1092–1097 (2021).

[50] Heinsohn, T. *et al.* Infection and transmission risks of COVID-19 in schools and their contribution to population infections in Germany: A retrospective observational study using nationwide and regional health and education agency notification data. *PLoS Medicine* **19**, e1003913 (2022).

[51] Colosi, E., Bassignana, G., Barrat, A. & Colizza, V. Modelling covid-19 in school settings to evaluate prevention and control protocols (2022).

[52] Colosi, E. *et al.* Screening and vaccination against covid-19 to minimise school closure: a modelling study. *The Lancet Infectious Diseases* **22**, 977–989 (2022).

[53] Faucher, B. *et al.* Agent-based modelling of reactive vaccination of workplaces and schools against covid-19. *Nature Communications* **13**, 1414 (2022).

[54] Di Domenico, L., Pullano, G., Sabbatini, C. E., Boëlle, P.-Y. & Colizza, V. Modelling safe protocols for reopening schools during the covid-19 pandemic in france. *Nature Communications* **12**, 1073 (2021).

[55] Pham, T. M. *et al.* Seasonal patterns of sars-cov-2 transmission in secondary schools: a modelling study. *medRxiv* (2022).

[56] Prem, K. *et al.* Projecting contact matrices in 177 geographical regions: an update and comparison with empirical data for the COVID-19 era. *PLoS Computational Biology* **17**, e1009098 (2021).

[57] Wong, K. L. *et al.* Social contact patterns during the COVID-19 pandemic in 21 European countries–evidence from a two-year study. *BMC Infectious Diseases* **23**, 268 (2023).

[58] Verelst, F. *et al.* SOCRATES-CoMix: a platform for timely and open-source contact mixing data during and in between COVID-19 surges and interventions in over 20 European countries. *BMC Medicine* **19**, 254 (2021).

[59] Lauer, S. A. *et al.* The incubation period of coronavirus disease 2019 (COVID-19) from publicly reported confirmed cases: estimation and application. *Annals of Internal Medicine* **172**, 577–582 (2020).

[60] Park, M., Cook, A. R., Lim, J. T., Sun, Y. & Dickens, B. L. A systematic review of COVID-19 epidemiology based on current evidence. *Journal of Clinical Medicine* **9**, 967 (2020).

[61] Ali, S. T. *et al.* Serial interval of SARS-CoV-2 was shortened over time by nonpharmaceutical interventions. *Science* **369**, 1106–1109 (2020).

[62] Santamaría, L. & Hortal, J. Chasing the ghost of infection past: identifying thresholds of change during the covid-19 infection in spain. *Epidemiology & Infection* **148**, e282 (2020).

[63] Hicketier, A., Bremer, V. *et al. Wirksamkeit und Wirkung von anti-epidemischen Maßnahmen auf die COVID-19-Pandemie in Deutschland (StopptCOVID-Studie)* (Robert Koch-Institut, 2023).

[64] Kislaya, I. *et al.* Seroprevalence of SARS-CoV-2 infection in Portugal in May-July 2020: results of the first national serological survey (ISNCOVID-19). *Acta Medica Portuguesa* **34**, 87–94 (2021).

[65] Diekmann, O., Heesterbeek, J. & Roberts, M. G. The construction of next-generation matrices for compartmental epidemic models. *Journal of the Royal Society Interface* **7**, 873–885 (2010).

[66] de Kroon, H., Plaisier, A., van Groenendael, J. & Caswell, H. Elasticity: the relative contribution of demographic parameters to population growth rate. *Ecology* **67**, 1427–1431 (1986).

[67] Van Groenendael, J., De Kroon, H., Kalisz, S. & Tuljapurkar, S. Loop analysis: evaluating life history pathways in population projection matrices. *Ecology* **75**, 2410–2415 (1994).

[68] Gabinetes da Secretária de Estado Adjunta e da Educação e do Secretário de Estado da Educação. Diário da República, 2.ª série — N.º 115 — 18 de junho de 2019 (2019). URL https://files.diariodarepublica.pt/2s/2019/06/115000001/0000200005.pdf.